PRODUCTION OF ACTIVATED CARBON DERIVED FROM RICE HULLS USING SUGAR CANE BAGASSE AS ACTIVATING AGENT

by

Pegah ABDOLKARIMI

THESIS PRESENTED TO ÉCOLE DE TECHNOLOGIE SUPÉRIEURE
IN PARTIAL FULFILLMENT OF A MASTER'S DEGREE
WITH THESIS IN ENVIRONMENTAL ENGINEERING
M.A.Sc.

MONTREAL, FEBRUARY ,23 ,2024

ÉCOLE DE TECHNOLOGIE SUPÉRIEURE
UNIVERSITÉ DU QUÉBEC

BOARD OF EXAMINERS

THIS THESIS HAS BEEN EVALUATED

BY THE FOLLOWING BOARD OF EXAMINERS

M. Frédéric Monette, Thesis supervisor
Department of Construction Engineering, École de technologie supérieure

Ms. Josiane Nikiema, President of the board of examiners
Department of Construction Engineering, École de technologie supérieure

M. Mathieu Lapointe, External examiner
Department of Construction Engineering, École de technologie supérieure

THIS THESIS WAS PRESENTED AND DEFENDED

IN THE PRESENCE OF A BOARD OF EXAMINERS AND THE PUBLIC

ON FEBRUARY 9,2024

AT ÉCOLE DE TECHNOLOGIE SUPÉRIEURE

ACKNOWLEDGEMENTS

I would like to express my gratitude to Professor Frédéric Monette, my thesis advisor from the Department of Civil and Environmental Engineering. Throughout the process of writing this thesis, Prof. Monette provided invaluable guidance, offering suggestions for improvement, and steering me in the right direction whenever necessary. Next, I wish to express my heartfelt appreciation to my family. Despite the physical distance that separated me from my home, I carried each one of you in my thoughts and held you close to my heart. I began with my father, mother, and sister for their unwavering support throughout my academic journey, for their extraordinary love and care, and for the unwavering belief and confidence they instilled in me. Additionally, I extend my appreciation to the laboratory personnel for their assistance in providing the required equipment and resources and providing the best atmosphere to finish my work.

PRODUCTION DE CHARBON ACTIF DÉRIVÉ DE COQUES DE RIZ EN UTILISANT LA BAGASSE DE CANNE À SUCRE COMME AGENT ACTIVATEUR

Pegah ABDOLKARIMI

RÉSUMÉ

La contamination généralisée des ressources naturelles en eau par des polluants constitue un défi environnemental majeur. Ce mémoire explore le potentiel du charbon actif dérivé de coque de riz en tant qu'adsorbant viable pour l'élimination des contaminants des solutions aqueuses, en se concentrant spécifiquement sur le bleu de méthylène en tant que solution modèle. L'étude présente une analyse complète des cinétiques d'adsorption, des isothermes et de leurs implications pour la remédiation environnementale. Elle implique la gazéification de la balle de riz en utilisant la bagasse de canne à sucre, un autre sous-produit agricole économique, comme source de dioxyde de carbone CO_2 dans un environnement riche en oxygène pour activer le carbone. Ce processus utilise une technique appelée méthode des deux creusets, qui réduit au minimum l'utilisation d'oxygène tout en utilisant le CO_2 comme agent activateur. Cette approche améliore le développement du charbon actif en augmentant sa porosité et en lui conférant une importante surface spécifique, le rendant ainsi adapté à diverses applications de traitement.

Les présents travaux ont montré que l'efficacité d'adsorption du bleu méthylène et de l'iode était maximale lorsque de la balle de riz a été soumises à un traitement chimique et physique avec HNO_3 et NaOH 1N pendant 2 heures à $710°C$ pendant 30 minutes, avec une vitesse de chauffage de $10°C \cdot min^{-1}$ et de la bagasse de canne à sucre comme agent activateur. Le charbon activé dérivé de la balle de riz a présenté un nombre d'iode de 836 $mg \cdot g^{-1}$, taux d'élimination du bleu de méthylène à 94.1% et sa capacité d'adsorption a été rapportée à 285 $mg \cdot g^{-1}$ à une température de $25°C$.

Les cinétiques d'adsorption ont été explorées en examinant le temps de contact et la concentration initiale du polluant. Les données expérimentales ont été ajustées à divers modèles cinétiques, notamment les modèles de pseudo-premier ordre, de pseudo-deuxième ordre, d'Elovich et de diffusion intraparticules. Les résultats d'adsorption du bleu de méthylène est en accord avec le modèle cinétique de pseudo-deuxième ordre ($R^2 > 0.99$), indiquant que la chimisorption est l'étape de contrôle. De plus, l'étude a évalué les isothermes d'adsorption en faisant varier les concentrations initiales du polluant. Les modèles d'isothermes de Langmuir, de Freundlich, de BET et de Temkin ont été appliqués à l'ensemble de données. Le modèle d'isotherme de Langmuir a montré le meilleur ajustement ($R^2 > 0.99$), suggérant une adsorption en monocouche avec un nombre fini de sites d'adsorption.

Cette recherche présente des implications pratiques pour la conception de systèmes de traitement de l'eau basés sur l'adsorption visant à éliminer les contaminants de l'eaux. Le charbon actif provenant de la balle de riz, renforcé par l'utilisation de la bagasse de canne à sucre en tant qu'agent physique, émerge comme un adsorbant prometteur qui implique un minimum de contraintes techniques. Les recherches futures pourront se pencher sur les stratégies d'optimisation de la production de charbon actif et sur la conception de systèmes d'adsorption à plus grande échelle.

Mots-clés: adsorption, production de charbon actif, balles de riz, la bagasse de canne, résidus agricoles, activation physique

PRODUCTION OF ACTIVATED CARBON DERIVED FROM RICE HULLS USING SUGAR CANE BAGASSE AS ACTIVATING AGENT

Pegah ABDOLKARIMI

ABSTRACT

Widespread contamination of natural water resources by pollutants poses a significant environmental challenge. This thesis explores the potential of activated carbon derived from rice husk as a viable adsorbent for eliminating contaminants from aqueous solutions, specifically focusing on methylene blue as a model solution. The study provides a comprehensive analysis of adsorption kinetics, isotherms, and their implications for environmental remediation. It involves the gasification of rice husk using sugarcane bagasse, another economical agricultural byproduct, as a source of carbon dioxide (CO_2) in an oxygen-rich environment to activate the carbon. This process utilizes the two crucible method minimizing oxygen use and using CO_2 as an oxidizing agent. This approach enhances activated carbon development by increasing its porosity and providing a substantial surface area, making it suitable for various treatment applications.

The present work demonstrated that the adsorption efficiency of methylene blue and iodine was maximum when rice husk underwent chemical and physical treatment with HNO_3 and NaOH 1N for 2 hours at $710°C$ for 30 minutes, with a heating rate of $10°C \cdot min^{-1}$, and sugarcane bagasse as the activating agent. The activated carbon derived from rice husk exhibited an iodine number of 836 $mg \cdot g^{-1}$, methylene blue removal rate at 94.1% and its adsorption capacity was reported as 285 $mg \cdot g^{-1}$ at a temperature of $25°C$.

Adsorption kinetics were explored by examining the contact time and initial concentration of the pollutant. Experimental data were fitted to various kinetic models, including pseudo-first-order, pseudo-second-order, Elovich, and intraparticle diffusion models. The results of methylene blue adsorption were in agreement with the pseudo-second-order kinetic model ($R^2 > 0.99$), indicating that chemisorption is the rate-controlling step. Additionally, the study evaluated adsorption isotherms by varying the initial concentrations of the pollutant. Langmuir, Freundlich, BET, and Temkin isotherm models were applied to the dataset. The Langmuir isotherm model showed the best fit ($R^2 > 0.99$), suggesting monolayer adsorption with a finite number of adsorption sites.

This research has practical implications for designing water treatment systems based on adsorption to eliminate water contaminants. Activated carbon from rice husk, enhanced by using sugarcane bagasse as an activating agent, emerges as a promising adsorbent with minimal technical constraints. Future research may focus on optimizing activated carbon production strategies and designing larger-scale adsorption systems."

Keywords: Adsorption, activated carbon production, agricultural residues, rice husk, sugarcane bagasse, physical activation

TABLE OF CONTENTS

LIST OF TABLES

LIST OF FIGURES

LIST OF ABBREVIATIONS

RH	Rice Husk
SCB	Sugarcane Bagasse
GAC	Granular Activated Carbon
AC	Activated Carbon
BET	Brunauer-Emmett-Teller
N_2	Nitrogen
MB	Methylene Blue
SEM	Scanning Electron Microscope
V	Volume of solution (L)
g	Grams
COD	Chemical Oxygen Demand
BOD	Biochemical Oxygen Demand

LIST OF SYMBOLS AND UNITS OF MEASUREMENTS

q_e	amount of absorbate in the absorbent at equilibrium ($mg \cdot g^{-1}$)
q_0	maximum monolayer coverage capacity ($mg \cdot g^{-1}$)
C_e	equilibrium concentration ($mg \cdot L^{-1}$)
b	Langmuir isotherm constant ($dm^3 \cdot mg^{-1}$)
n	adsorption intensity
T	temperature (K)
K_F	Freundlich isotherm constant ($mg \cdot g^{-1}$)
R	universal gas constant (8.314 $J \cdot mol^{-1} \cdot K^{-1}$)
b_T	Temkin isotherm constant
A_T	Temkin isotherm equilibrium binding constant ($L \cdot g^{-1}$)
ε	Dubinin-Radushkevich isotherm constant
q_s	theoretical isotherm saturation capacity ($mg \cdot g^{-1}$)
β	Dubinin-Radushkevich isotherm constant ($mol^2 \cdot kJ^{-2}$)
C_0	adsorbate initial concentration ($mg \cdot L^{-1}$)
θ	degree of surface coverage
n_{FH}	Flory-Huggin's isotherm model exponent
K_{FH}	Flory-Huggin's isotherm equilibrium constant ($L \cdot g^{-1}$)
K_D	Hill constant
q_{sH}	Hill isotherm maximum uptake saturation ($mg \cdot L^{-1}$)

n_H	Hill cooperativity coefficient of the binding interaction
K_R	Redlich-Peterson isotherm constant ($L \cdot g^{-1}$)
a_R	Redlich-Peterson isotherm constant ($1 \cdot mg^{-1}$)
g	Redlich-Peterson isotherm exponent
K_s	Sips isotherm model constant ($L \cdot mg^{-1}$)
β_s	Sips isotherm model exponent
K_T	Toth isotherm constant ($L \cdot mg^{-1}$)
t	Toth isotherm constant
A	Koble-Corrigan isotherm constant ($L^n \cdot mg^{1-n} \cdot g^{-1}$)
B	Koble-Corrigan isotherm constant ($L \cdot mg^{-1n}$)
α_k	Khan isotherm model exponent
β_k	Khan isotherm model constant
α_{RP}	Radke-Prausnitz isotherm model constant
γ_R	Radke-Prausnitz isotherm model constant
β_R	Radke-Prausnitz isotherm model exponent
a	Frenkel-Halsey-Hill isotherm constant ($I \cdot m^{-r} \cdot mole^{-1}$) with r (sign of the inverse power)
d	Interlayer spacing (m)
k	MacMillan-Teller (MET) isotherm constant
R_L	Dimensionless separation factor
K_f	Freundlich isotherm constant related to adsorption capacity ($mg \cdot g^{-1}$)

k_2	Rate constant of second-order adsorption ($g \cdot mg^{-1} \cdot min^{-1}$)
k_1	Rate constant of first-order adsorption ($1 \cdot min^{-1}$)
b	Adsorption energy constant of Langmuir adsorption isotherm ($L \cdot mg^{-1}$)
n	Freundlich isotherm constant related to adsorption capacity
R^2	Coefficient of Determination
C_0	Initial Concentration
C_e	Equilibrium Concentration
Q	Maximum Adsorption Capacity ($mg \cdot g^{-1}$)
Q_{max}	Maximum Adsorption Capacity ($mg \cdot g^{-1}$)
W	Mass of adsorbent (g)

INTRODUCTION

In contemporary times, due to increasing demands for water resources and environmental protection, It is essential to take into account the scarcity of water, reduce water usage, and recycle or reuse water on a regular basis. Also, it is of paramount importance to minimize wastewater pollution from various uses. Domestic, industrial, and agricultural activities and water resource consumption add up to multiple contaminants and pollutants, which cause diseases and should be restricted from human use (Kao et al., 2008) These activities significantly encompass one-third of the available water resources (René Schwarzenbach and Wehrli, 2010). Water contamination has become a problem for human beings and other aquatic living organisms, and the environment (René Schwarzenbach and Wehrli, 2010).

The presence of inorganic pollutants (e.g., heavy metal ions) and organic pollutants (e.g., dyes) in water supplies is caused by various industries such as mines and metal plating facilities, paper industries, batteries, dying, and textiles Song, 2012. The low-concentrated presence of heavy metal ions and dye effluents in industrial waste types can make their discharge into drinking water difficult and demanding (Singh, 2018). Several treatment technologies have been introduced and studied for wastewater treatment for years (Goyal, 2005).

These treatment methods are divided into physical, chemical, and biological methods. They can be employed to eliminate various pollutants from water, namely, flocculation/coagulation, biological oxidation, photo-Fenton treatments, advanced oxidation process (AOPs), oxidation using chemical oxidants (hydrogen peroxide, ozone, etc.), membrane processes, electrochemical oxidation and degradation, and adsorption. Also, some of these treatment techniques can be integrated for optimum efficiency in adsorption capacity as well. The adsorption process through activated carbon is a convenient mode to eliminate pollutants in water due to its cost-effectiveness, simplicity in design and setup (Fu and Wang, 2011). This technology is commonly employed for water treatment since it has been mentioned in numerous papers. The disadvantage the

adsorption process has over other treatment methods is its incapability to remove bacteria and microbes. However, other treatments such as membrane filtration, oxidation, ion exchange and electrochemical processes require a high initial cost of operation and most of them have hazardous residual wastes and sludges which are costly to eliminate (Singh, 2018).

The central aim of this investigation is to devise an innovative, less technically restrained, and environmentally sustainable methodology for the synthesis of activated carbon derived from agricultural residues such as rice husk while minimizing technical constraints. The principal focus of this study is the investigation of efficiency of the produced activated carbon through the utilization of agricultural residue, specifically sugarcane bagasse, as a physicochemical agent to optimize the production environment for activated carbon synthesis. Additionally, chemical impregnation is incorporated into the production process to augment the surface characteristics of the resulting activated carbon.

The literature review chapter surveys existing scholarly works and scientific literature, providing a comprehensive synthesis of the current state of knowledge pertaining to activated carbon production methodologies, with a specific emphasis on those involving agricultural residues. This chapter examines previous studies, identifies gaps in the existing literature, and lays the theoretical foundation for the subsequent chapters.

Moving forward, the material and methods chapter outlines the experimental design and procedures employed in this investigation. It shows the step-by-step process of utilizing sugarcane bagasse as a key component in the production of activated carbon from rice husk, with a focus on maintaining a cost-effective and environmentally friendly approach under atmospheric conditions. The results and discussion chapters unveil the outcomes of the experimental setup, presenting a detailed analysis of the activated carbon produced. Furthermore, a thorough investigation into the isotherm and kinetic studies has been conducted on the activated carbon generated through this innovative methodology.

CHAPTER 1

LITERATURE REVIEW

The adsorption process becomes a key component in the field of water treatment in the search for safe and clean water. For communities all across the world, having access to clean drinking water is an essential requirement, so we must investigate practical ways to eliminate pollutants. This literature review begins with a thorough analysis of the adsorption process, an important and frequently utilized method in water treatment. This chapter provides the foundation for a thorough investigation of its function in resolving water quality issues and advancing environmental engineering by analyzing its principles and uses.

1.1 Adsorption phenomenon

Every solid or liquid surface contains molecules, and when the forces in the molecules are not balanced and saturated enough, the adsorption phenomenon materializes. Therefore, the contact between solid's or the liquid's surface (adsorbent) with liquid or gas, the surface molecular forces interact with the liquid or the gas molecular forces (adsorbate). The substance that accumulates on the surface is the adsorbate, and adsorption happens on the substance's surface, named the adsorbent (Singh, 2018). Adsorption is a mass transfer process in which components collect at the interface between two phases: gas–solid, absorption, liquid-solid, or liquid–liquid interface. The characteristics of adsorbates and adsorbents are rather specific and are dependent on their molecular components.

Physisorption usually happens when the adsorbed molecules naturally interact with the solid surface. It occurs when comparatively weak van der Walls forces attach the adsorbate to the surface (Goyal, 2005). Besides that, chemisorption occurs when the forces of attraction between adsorbed molecules and the solid surface area happen due to chemical bonding.

Because chemisorption only occurs as a monolayer, substances chemisorbed on a solid surface are difficult to eliminate due to more vital forces/bonds. In this process, the adsorbate molecules

and the adsorbent surface share and exchange electrons, which induce a chemical reaction (Singh, 2018; Worch, 2012). As can be seen, Figure 1.1 presents the important terms of an adsorption process.

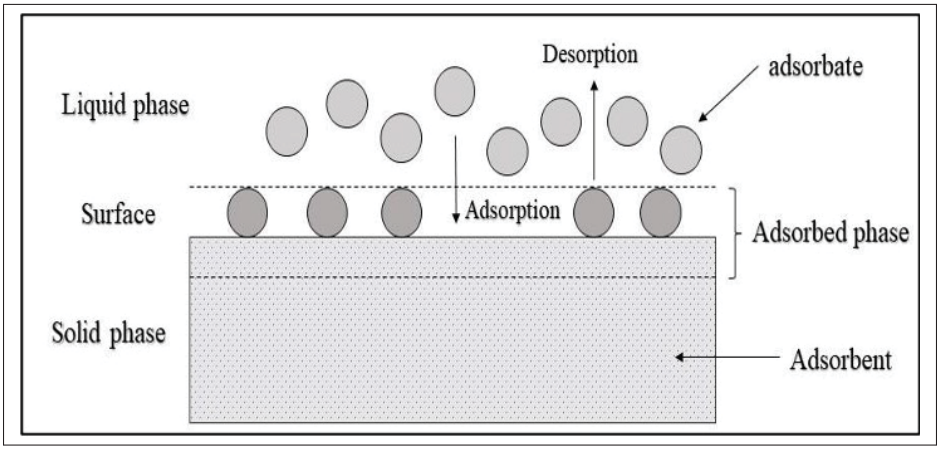

Figure 1.1 Terms of the adsorption various phases (taken from Zietzschmann et al., 2014)

1.2 Adsorption kinetics mechanism

Moving molecules from a high concentration area to a low concentration area is known as diffusion. Diffusion affects the rate at which molecules can bind to the substance's surface during the adsorption process. Adsorption rates can accelerate with increased diffusion rates. The adsorption process and diffusion analysis can lead to a wide variety of models that are both systematic and nuanced (Yakout, 2014). Generally, an adsorption kinetic model has three essential input data which are mentioned in Figure 1.1 (Worch, 2012): mass transfer equations, equilibrium correlations for the employed reactor. Moreover, kinetic models (Figure 1.2) typically consist of basic premises such as:

a) Constant temperature,
b) Thoroughly mixed bulk solution,
c) The adsorbent's internal mass transfer can be explained as a diffusion process,
d) Compared to the diffusion process rate,
e) The shape of the adsorbent must be rounded and isotropic (Worch, 2012).

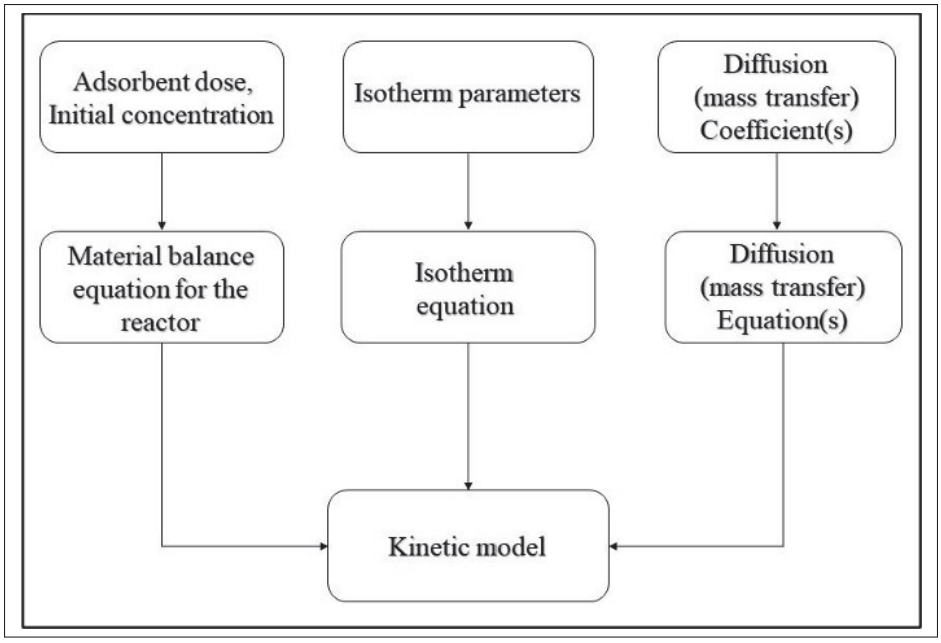

Figure 1.2 Kinetic model parameters and their relation (taken from Zietzschmann et al., 2014)

1.3 Adsorption isotherm models

An adsorption isotherm is a curve that defines the phenomenon in which the release or retention of a substance in an aquatic environment to a solid-phase substance along with steady temperature and pH materializes (Sawyer, 2003). In this context, equilibrium relationships, also known as adsorption isotherms, define how contaminants interact with adsorbent materials and are thus essential to optimizing adsorption mechanism routes, describing the surface properties and capacities of adsorbents, and implementing appropriate adsorption systems (Pokhrel, 2004); El-Khaiary, 2008). A broad category of equilibrium isotherm models in terms of three principal approaches , nonlinear form, linear form and plot are developed over years, as shown in Table 1.1 (Singh, 2018) and the constants of each isotherm model are written below the table.

Table 1.1 Isotherm models linear and nonlinear forms

Isotherm	**Nonlinear form**	**Linear form**
Langmuir	$q_t = \frac{q_0 b C_e}{1+bC_e}$ $\frac{q_e}{C_e} = bQ_0 - bq_e$	$q_e = Q_0 - \frac{bq_e}{1+bq_e}$ $\frac{1}{q_e} = \frac{1}{Q_0} + \frac{1}{bQ_0 C_e}$
Freundlich	$q_e = K_f C_e^{1/n}$	$\log q_e = \log K_f + \frac{1}{n} \log C_e$
Dubinin-Radushkevich	$q_e = q_s \exp(-k_{ad}\varepsilon^2)$	$\ln q_e = \ln(\ln q_s) - k_{ad}\varepsilon^2$
Temkin	$q_e = \frac{RT}{b_T} \ln A_T C_e$	$q_e = \frac{RT}{b_T} \ln A_T + \frac{RT}{b_T} \ln C_e$
Flory-Huggins	$\frac{\theta}{C_0} = K_{FH}(1-\theta)^{n_{FH}}$	$\log\left(\frac{\theta}{C_0}\right) = \log K_{FH} + n_{FH} \log(1-\theta)$
Hill	$q_e = \frac{q_s^H C_e^n}{K_D + C_e^n}$	$\log\left(\frac{q_e}{q_s^H - q_e}\right) = n_H \log(C_e) - \log K_D$
Redlich-Peterson	$q_e = \frac{K_R C_e}{1+a_R C_e^g}$	$\ln\left(\frac{K_R C_e}{C_e - 1}\right) = g \ln(C_e) + \ln a_R$
Sips	$q_e = \frac{K_s C_e^{\beta_S}}{1+a_S C_e^{\beta_S}}$	$\beta_S \ln(C_e) = -\ln\left(\frac{k_s}{q_e}\right) + \ln a_S$
Toth	$q_e = \frac{K_T C_e}{(a_T + C_e)^{1/t}}$	$\ln\left(\frac{q_e}{K_T}\right) = \ln(C_e) - \frac{1}{t} \ln(a_r + C_e)$
Koble-Corrigan	$q_e = \frac{AC_e^n}{1+BC_e^n}$	$\frac{1}{q_e} = \frac{1}{AC_e^n} + \frac{B}{A}$
Khan	$q_e = \frac{q_S b_k C_e}{1+b_k C_e}$	-
Radke-Prausnitz	$q_e = \frac{a_{RP} r_R C_e^{\beta_R}}{a_{RP} + r_R C_e^{\beta_R - 1}}$	-
Frenkel-Halsey-Hill	$\ln\left(\frac{C_e}{C_S}\right) = -\frac{\alpha}{RT}\left(\frac{q_s}{q_e - d}\right)^r$	-
Mac Milla-Teller	$q_e = q_s \left(\frac{k}{\ln\left(\frac{C_s}{C_e}\right)}\right)^{1/3}$	-

The terms are defined in the symbols section.

There are several different forms of adsorption isotherms (Adamson, 1997). However, The Langmuir and Freundlich isotherms are the most prominent ones. The Langmuir isotherm curve has a preliminary slope that is proportional to the rate of alteration of available active sites on the particle, with growing solute adsorption to the sites. If enough solute is adsorbed, the likelihood of additional species finding an adsorption site reduces, and the curve reaches a plateau (Giles, 1960). In the same way that the Langmuir equation provides a visual analysis of the volume of solute adsorbed on the surface of the substrate, the Freundlich equation does.

The Langmuir adsorption isotherm, on the other hand, gives the sum of solute adsorbing in the form of a monolayer on the adsorbent's external surface. As a result, it theoretically describes the ion distribution equilibrium between the solid and liquid phases. The Freundlich adsorption isotherm defines the liquid-solid interface's adsorption behavior. The first approach can be considered kinetic, where the state of adsorption equilibrium is defined as a state of dynamic equilibrium. In dynamic equilibrium, adsorption and desorption rates are similar. The second approach (Freundlich adsorption isotherm) refers to the thermodynamics that various adsorption models can originate from its structure. It may originate from the Langmuir isotherm by considering that there is a dispersion of sites on the adsorbent with various affinities for different adsorbates and that each site follows the Langmuir isotherm Sawyer, 2003.

1.3.1 Langmuir isotherm model

The Langmuir is an isotherm model characterized by two parameters. It was formulated under the premise that all active sites involved in the adsorption process exhibit equivalent binding affinities. This model represents the adsorbent surface as uniform in nature (Langmuir, 1916). After applying the initial and final boundary conditions, the linear expression of the Langmuir equation is presented below:

$$\frac{C_e}{q_e} = \frac{C_e}{q_1} + \frac{1}{b_1 q_1} \tag{1.1}$$

Where:

q_e = the experimental adsorption capacity at equilibrium (mg·L^{-1}),

C_e = equilibrium adsorbate concentration (mg·L^{-1}),

b_1 = Langmuir constants (L^{-1}·mg^{-1}),

q_1 = maximum adsorption capacity (mg·g^{-1})

In this isotherm model, the constant values can be extracted by analyzing the intercept and slope of the graph $\frac{C_e}{q_1}$ against C_e.

1.3.2 Freundlich isotherm model

The Freundlich isotherm, a two-parameter model, effectively captures adsorption onto a surface with heterogeneous characteristics. Within this isotherm, the initial stages of the adsorption process generally involve the occupancy of more potent binding sites, followed by a gradual decline in binding affinity (Freundlich, 1907). The linear representation of the Freundlich equation is as follows:

$$\log(q_e) = \log(K_f) + \frac{1}{n_f}\log(C_e) \tag{1.2}$$

Where:

k_f = Freundlich isotherm constants $(mg \cdot g^{-1}) \cdot (mg^{-1} \cdot L^{-1})^{-n}$

n_f = Freundlich exponent$(dimensionless)$

These constants can be calculated from the slope and the intercept of the plot $\log(q_e)$ versus $\log(C_e)$.

1.3.3 BET isotherm model

One of the most effective isotherm models for expressing adsorption phenomena is the BET isotherm, which Brunauer, 1938 created. This equation is firmly rooted in theory and offers

a comprehensive insight into the characteristics of adsorption processes. The model enables the exploration of multilayer adsorption patterns, monolayer adsorption capacities, and the heat associated with adsorption at different layers, thereby providing a means to ascertain various adsorption parameters. The isotherm model facilitates the determination of parameters related to adsorption, including the behavior of multilayer adsorption, monolayer adsorption capacity, and the heat of adsorption across different adsorption layers (Ebadi, 2009).

This model postulates the accumulation of multiple layers of adsorbate on the surface, with the application of the Langmuir isotherm to each layer. It introduces a degree of complexity beyond that of the Langmuir isotherm. The BET equation can be expressed in the subsequent format:

$$\frac{C}{q(C_s - C)} = \frac{1}{bq_m} + \frac{b-1}{bq_m}\frac{C}{C_s} \tag{1.3}$$

Where:

C_s = saturation concentration of the adsorbate in the solution ($mg \cdot g^{-1}$)

Utilizing this equation, the parameters C_s and b can be derived by analyzing the gradient and intercept of the linear fit applied to the plot involving the left side of the equation against C/C_s (Sawyer, 2003).

1.3.4 Temkin isotherm model

To characterize adsorption processes, especially on heterogeneous surfaces, the Temkin isotherm model is another frequent equation. Temkin isotherm: Adsorbent-adsorbate interactions cause all molecules in the layer's heat of adsorption to decrease linearly with coverage. Plotting the experimental data yields a linear plot like the Freundlich isotherm, from which the Temkin isotherm constants can be calculated. In adsorption studies where the interactions between the adsorbate and the adsorbent are not solely physical or chemical, this model is particularly helpful. Understanding the energetics of adsorption processes and the nature of adsorption on

surfaces with different energetics is made easier with the help of the Temkin isotherm(Annable, 1952). Temkin isotherm equation can be expressed in the following linear form:

$$q_e = B \ln(AC_e) \tag{1.4}$$

Where:

q_e = Solute adsorbed per unit mass of the adsorbent at equilibrium ($mg \cdot g^{-1}$),

B = Temkin isotherm constant related to the adsorption heat ($J \cdot mol^{-1}$),

A = Temkin isotherm constant related to equilibrium binding ($L \cdot g^{-1}$).

1.4 Kinetic models of Adsorption

It is worth mentioning that kinetic models can be practiced if the imperative equilibrium parameters exist. Accordingly, it can be implied that the adsorption kinetics does not rely on the adsorption equilibrium. In the table below (Table 1.2), the kinetic models are presented in six different orders (Çiftçi Henden, 2015; Benjelloun, 2021).

Table 1.2 Kinetic models linear and nonlinear forms

Model names	**Equations**	**Straight line plot**
Pseudo-first order	$\log(q_e - q_t) = \log(q_e) - \frac{k_1}{2.303}t$	$\log(q_e - q_t)$ vs. t
Pseudo-second order	$\frac{t}{q_t} = \frac{1}{k_2 q_e^2} + \frac{t}{q_e}$	$\frac{t}{q_t}$ vs. t
Elovich	$q_t = \beta \ln(\alpha\beta) - \ln t$	q_t vs. $\ln t$
Intra-particle diffusion	$q_t = K_p t^{0.5} + C$	q_t vs. $t^{0.5}$
Boyd kinetic model	$B_t = -0.4977 - \ln(1 - \frac{q_t}{q_0})$	B_t vs. t
Bangham's model	$\log(\log(C_t/C_0 - q_t^m)) = \log(k_0) + q_t \log t$	$\log(\log(C_t/C_0 - q_t^m))$ vs. $\log t$

Where:

q_e = amount of absorbate in the absorbent at equilibrium ($mg \cdot g^{-1}$),

q_t = amount of absorbate in the absorbent at equilibrium at time t ($mg \cdot g^{-1}$),

C_0 = initial concentration of the adsorbate ($mg \cdot L^{-1}$),

C_t = initial concentration of the adsorbate at time t ($mg \cdot L^{-1}$),

k_1, k_2, k_p = the constant (t^{-1}).

1.4.1 Pseudo-first-order kinetic model

The adsorption rate is a crucial factor in determining how well-tested adsorbents perform during the adsorption process. The rate constants, initial adsorption rates, and adsorption capacities of the synthesized activated carbons were estimated using the pseudo-first- and pseudo-second-order kinetic models to examine the controlling mechanism of the adsorption process.

The Shahwan, 2015 suggested for characterizing the adsorption process in liquid-solid systems. The nonlinear variant of this model is expressed by the subsequent equation:

$$\frac{dq_t}{dt} = k_f(q_e - q_t) \tag{1.5}$$

The pseudo-first-order model changes to the following linear equation after taking into consideration the initial and final boundary conditions (t=0 - t and q_t= 0- q_t) (Sparks, 1991):

$$\log(q_e - q_t) = \log(q_e) - \frac{k_f}{2.303}t \tag{1.6}$$

Where:

q_t = the adsorbent amount adsorbing the adsorbate solution at time t ($mg \cdot g^{-1}$),

q_e = the adsorption capacity of the adsorbate at the time of equilibrium ($mg \cdot g^{-1}$),

k_f = pseudo-second-order constant (t^{-1}),

The constant that can be calculated from the plot $\log(q_e - q_t)$.

1.4.2 Pseudo-second-order kinetic model

This kinetic model was formulated grounded on the chemisorptive interaction occurring between the adsorbate and the adsorbent surface, encompassing van der Waals forces through electron exchange. Following the inclusion of boundary conditions (t=0-t and q_t=0-q_t), the equation takes on a linear format as presented below:

$$\frac{t}{q_t} = \frac{1}{k_s q_e^2} + \frac{1}{q_e} t \tag{1.7}$$

Where:

K_s = the constant value at equilibrium (t^{-1}).

1.4.3 Intra-particle diffusion kinetic model

The diffusion model examines the movement of the adsorbate from the solution into the pores of the adsorbent, serving as the limiting factor for the rate of the process (Aravindhan, 2007;Haug, 1991). The Intraparticle diffusion kinetic model is represented as follows (Allen, 1989):

$$q_t = k_p t^{1/2} + C \tag{1.8}$$

Where:

q_t = adsorbed quantity at a given time t ($mg{\cdot}g^{-1}$),

k_p = rate constant for intraparticle diffusion ($mg{\cdot}g^{-1} \cdot h^{0.5}$),

C = boundary layer thickness constant ($mg{\cdot}g^{-1}$).

To examine the diffusion within the adsorption process, the kinetics data was graphed as q_t against the square root of time ($t^{0.5}$). The rate constant k_p was then determined from the gradient of the linear plots (q_t versus $t^{0.5}$).

1.4.4 Elovich kinetic model

In this model, The Elovich equation assumes that the solid surfaces involved in the adsorption process possess a range of different energy levels, and it also assumes that, under conditions of low surface coverage, neither desorption nor interactions between the adsorbed substances significantly influence the speed at which adsorption occurs. While the impact of surface energy diversity on adsorption equilibrium in gas-solid systems has been established, its applicability to liquid-solid systems remains uncertain (Rudzinski et al., 1992).

The Elovich equation is as follows when the boundary conditions $q=q_t$ at $t=t$ and $q=0$ at $t=0$ are applied:

$$q_t = \frac{1}{\beta} \ln(1 + \alpha\beta t) \tag{1.9}$$

Where:

q_t = sorption capacity at a given time t ($mg{\cdot}g^{-1}$),

α = initial sorption rate ($mg{\cdot}g^{-1}min^{-1}$),

β = desorption constant ($g{\cdot}mg^{-1}$).

The adsorption process is constituted of three main steps (Figure 1.3) The film diffusion is the first step where the adsorbates begin to spread through the sorbent particles' external surface from an aqueous solution. In the next step, the Intraparticle diffusion stage, the pores on the particle's inner part, yield the adsorbate to enter from the exterior space. At the last step, the interior enthalpy of the process becomes stable. Finally, the adsorbate particles attach to the adsorbent's micro-pores, either chemical or physical interaction (Torres-Knoop, 2017). It is noteworthy to mention that the slowest stage among these steps determines the overall rate of adsorption (Devi, 2020).

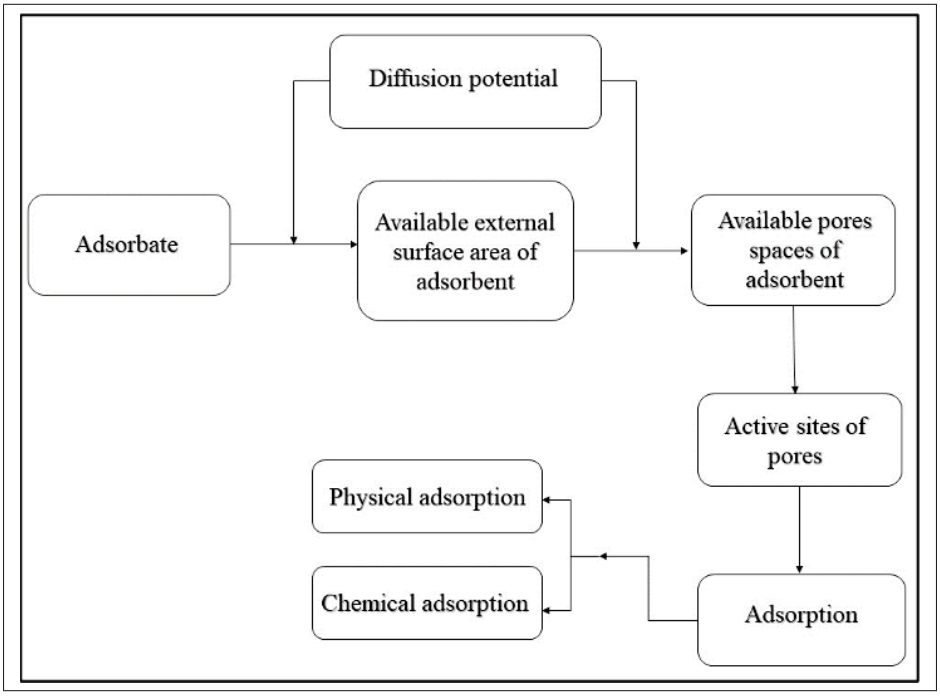

Figure 1.3 Comprehensive insight into the three stages of the adsorption process (taken from Hashtroudi, 2020)

1.5 Influential factors in the adsorption process

In the decontamination of water onto activated carbon via adsorption, prominent factors determine the adsorption rate and extent. One of the main factors that affect both the rate, and the extent of the adsorption is the molecules' features as being adsorbate and adsorbents (Sawyer,

2003). The solubility of a substance in water is another factor that impacts the extent of the adsorption; a substance with less solubility has more potential to be adsorbed (Sawyer, 2003).

Table 1.3 Water Purification Techniques

Technique	**Advantages**	**Disadvantages**	**References**
Coagulation	- Simple process - Cost-effective - Remove multiple pollutants - Uses low-cost chemical materials	- Chemicals should be added during the process - Trained and skilled operator needed - Produces hazardous waste sludge - Lengthy procedure	(Yan et al., 2008)
Membrane Filtration	- Eliminates all toxins, including micropollutants - Reusable - Low use of energy	- Unable to eliminate selected pollutants - Hazardous cleaning solution waste	(Wagner et al., 2001)
Oxidation	- Removes many organic contaminants - Can eliminate several heavy metals	- Operational costs are high - By-products of organic and inorganic oxidation	(Fiessinger et al., 1981)
Ion Exchange	- Fast result - Simple installation - Easy waste disposal	- In most cases, low pH is ineffective - Ineffective for high contaminant concentrations - Ineffective for extracting a mixture of metals - Initial maintenance costs and energy usage are also high	(Liberti and Helfferich, 1963)

Table 1.3 Water Purification Techniques (continued)

Technique	Advantages	Disadvantages	References
Electrochemical	- High-quality electricity. - Environmentally friendly and multifunctional.	- High initial operational cost and energy consumption - Mass transfer restrictions between the electrodes - Residual pollutants must be removed from the cathode	(Chen et al., 2011)
Chemical Precipitation	- Heavy metals are removed from polluted water.	- The method produces sludge, which must be disposed of.	(Kurniawan et al., 2006)
Reverse Osmosis	- Can eradicate odors or colors, as well as toxic metals and minerals. - Just about 5% of the water that passes through them is recovered; the rest is discharged as wastewater.	- Unless treated water storage systems are fumigated regularly, bacteria can multiply.	(Greenlee et al., 2009)
Adsorption	- An effective approach for removing heavy metals and organic compounds using a low-cost, environmentally friendly approach with a clear design and procedure.	- Unable to remove bacteria and microbes.	(Faust and Aly, 2013)

The substance's relative affinity explained as the equilibrium constant describing the equilibrium activities between two phases in a component, is another major factor. Since the adsorbate must infiltrate through the adsorbent's pores, the molecule's size is of paramount importance. his factor also impacts the diffusion rate to a surface in adsorption except for adsorption dealing with exchanging ions that are less inclined to be adsorbed than biological species (Sawyer, 2003).

Contact time is another critical component in the adsorption process (Shafiq, 2018). When the adsorbent particle size is smaller, it is simpler for the adsorbent to be attached to adsorbate through the adsorption process due to its capability to minimize internal diffusion and mass transfer constraints. Besides, the adsorbents with a small surface area face constraints with

the adsorbate's larger molecules, which causes a more extended contact time for acquiring the desired result in the adsorption process (Kyzas, 2014).

pH is also a determinant factor. Where the pH range is maintained in neutral, the adsorption rate is enhanced (Sawyer, 2003). Moreover, extra active convertible adsorption sites are supplied if the dosage of the adsorbents increases. On the other hand, the adsorption rate can be reduced due to the intrusion of redundant interaction of high amounts of adsorbent dosage (Shafiq, 2018). Table 1.3 exhibits various wastewater treatment techniques which are explained in the next page. Thermodynamic parameters ΔG°, ΔH°, and ΔS° define the potential nature of the adsorption process. Thus, thermodynamic parameters can predict the mechanisms of physical or chemical adsorption, and it can determine the temperature range in which the adsorption process has desired outcomes (Rudi et al., 2020). In the adsorption process, another influential factor that contributes to the estimation of thermodynamic parameters is temperature.

The relationship of ΔG° to enthalpy change ΔH° and entropy change ΔS° of adsorption is shown as:

$$\Delta G^\circ = \Delta H^\circ - T\Delta S^\circ \tag{1.10}$$

$$\Delta G^\circ = -RT \ln K \tag{1.11}$$

Where:

ΔG°: Gibbs free energy change, measured in (J) or (kJ). It represents the maximum reversible work that can be done by a system at constant temperature and pressure.

ΔH°: Enthalpy change, measured in (J) or (kJ). It represents the heat absorbed or released during a chemical or physical process at constant pressure.

T: Absolute temperature, measured in kelvin (K). The temperature is expressed on the Kelvin scale to ensure a positive value in the Gibbs equation.

ΔS°: Entropy change, measured in ($\mathrm{J{\cdot}K^{-1}}$) or ($\mathrm{J{\cdot}K^{-1}}$). It represents the measure of disorder or randomness in a system.

A negative Gibbs free energy value suggests that the adsorption process is viable and spontaneous (Din et al., 2014).

1.6 Use of adsorption technique

Elimination of organic substances such as products with taste and odour and other organic compounds in water, wastewater, and air is the primary application of adsorption in environmental prospects. Adsorption as a remediation method is applied in decreasing organic compounds such as trihalomethanes, pesticides, chlorinated compounds in drinking waters, and residuals in treated effluents and treatment of different industrial wastewater leachates (Jjagwe et al., 2021.

Several wastewater treatment technologies, such as flocculation/coagulation, oxidation process, membrane filtration, and adsorption, have been invented to reduce the contamination of organic substances in industrial wastewater (Table 1.3). However, through years of investigations, the adsorption process is reported to be the most economical and simple-designed mode, and the instructions are uncomplicated to operate (Abatan et al., 2019). Moreover, there are unlimited possibilities for the adsorption process to improve and be used to a broader extent (Saleem et al., 2019).

Based on the information provided in Table 1.3, chemical precipitation is a very effective and commonly used industrial technique in the removal of heavy metals and in a chemical precipitation process containing hydroxide precipitation and sulphide precipitation. Also, because of many advantages, such as high treatment capacity, high removal efficiency, and quick kinetics, ion-exchange techniques have been widely utilized to remove heavy metals from wastewater. Membrane filtering technologies using various types of membranes have a lot of potential for heavy metal removal due to their high efficiency, ease of use, and small footprint. However, it may contain hazardous cleaning solution wastes (Fu and Wang, 2011).

The electrochemical process is also an environmentally friendly process. However, it has high initial operational costs and high energy consumption. Moreover, oxidation removes a wide range of organic contaminants, but it also requires high operational costs like the electrochemical

process. Coagulation is one of the most important waste-water treatment procedures, although only the hydrophobic colloids and suspended particles are the main targets of coagulation. Therefore, it produces hazardous waste sludges which are hard to dispose of. Adsorption is a cost-effective and efficient approach for treating heavy metal effluent. It is versatile in terms of design and operation, and it produces high-quality treated effluent in many circumstances (Fu and Wang, 2011).

1.7 Methylene Blue test for adsorption study

Methylene blue can be used as a model for visual pollution and as an indicator of mesoporosity, hence adsorption studies using it are frequently employed to assess adsorbents. It is frequently employed as a dye in numerous contexts, such as colouring biological tissues, identifying chemical compounds, and as an indicator in chemistry research. Methylene blue is used as a drug to treat methemoglobinemia, a condition in which hemoglobin cannot carry oxygen properly, as well as a prospective treatment for a few neurological problems. Methylene blue is also used as a dye (Paciullo et al., 2010). The highest amount of dye that may be adsorbed on 1.0 g of adsorbent is called the methylene blue number. In the literature, it is referred to as q_{eq} (Paciullo et al., 2010).

Table 1.4 Properties of Methylene Blue (MB) (taken from Abdulmagid Basheer Agila et al., 2022)

Item	Methylene Blue (MB)
Trade Name	Desmoid piller, desmoidpillen, urelene blue, vitableu
Molecular Formula	$C_{16}H_{18}N_3SCl$
Density	1.0 g·mL^{-1} at 20°C
Wavelength (nm)	The maximum absorption of light is near 670 nm
Molecular Weight	319.86 g·mol^{-1}
pH	3 in water (10 g·L^{-1}) at 25°C

Isotherm and kinetic modes can be characterized which describes the adsorption of gasses or solutes onto solid surfaces of rice husk-activated carbon. It is predicated on the notion that adsorption takes place on an even surface with a certain number of similar sites that are

either occupied or vacant. There are several steps to perform batch adsorption to determine the isotherm and kinetic parameters of the produced activated carbon.

1.8 Preparation of activated carbon

An excellent adsorbent is activated carbon with a large surface area and high mesoporous volume (Danish and Ahmad, 2018). For the development of activated carbon (AC), two main ways are considered: pyrolysis of the raw material below 800°C (Alaya et al., 2000; Zondlo and Velez, 2007), and physical and chemical activation of the material with carbon content.

Pyrolysis is an energy recovery method that can yield the production of char, oil, and gas (Pütün et al., 2005). The particle size, temperature, and heating rate are the specific process parameters that have the greatest impact on the pyrolysis products.

In the first step, in physical activation which is a two-step process, the carbonaceous raw material is required to be carbonized under temperatures of 800°C (ranges between 400°C and 850°C) in a dormant situation which results in char production employing proper oxidizing gases, namely carbon dioxide, steam, and air, or their mixtures for the activation process. In the activation process, the temperature ranges between 600°C to 900°C (Goyal, 2005; Ioannidou and Zabaniotou, 2007). CO_2 is commonly considered the activation agent since it is safe, simple to handle, and allows for better control of the activation process due to its slow reaction at temperatures around 800°C (Goyal, 2005). The reason for dehydration is to prevent tar formation, which is not likely appropriate for the carbonization process (Lee et al., 2019).

On the other hand, chemical activation has many benefits, including the ability to combine carbonization and activation in a single step as the chemical activating agents such as $ZnCl_2$, KOH, H_3PO_4, and K_2PO_3 as dehydrating agents are mixed with a precursor (Ateş and Özcan, 2018). Also, it can conduct it at lower temperatures, resulting in generating a more desirable porous structure. However, using chemical agents for activation can cause many environmental issues. The cost of chemicals is a key disadvantage of the chemical activation method (Table

1.5), and it necessitates an additional step of flushing activated carbon with hot and cold water to remove unreacted chemicals and chemical by-products (Danish and Ahmad, 2018).

The raw material is treated with chemical agents such as nitric acids, sulphuric acids, sodium acids, zinc chloride, phosphoric acid, etc. at different temperatures throughout the process as it is mentioned in Table 1.6 (Mohammadi et al., 2021; Lee et al., 2019) It should be noted that,. Nevertheless, the carbonaceous materials have the potential to be converted into activated carbon (Goyal, 2005).

Table 1.5 Types of activation methods and activating agents for agricultural materials (taken from Ioannidou and Zabaniotou, 2007)

Activation Method	**Steps of Process**	**Used Material**	**Activating Agent**
Physical	Two-steps	- Olive residues - Rice husk - Rice straw - Pecan shells - Hazelnut shells - Peanut hulls	- Steam - CO_2 - Air
Chemical	One-step	- Olive seeds - Rice husks - Rice straw - Pecan shells - Hazelnut shells - Peanut hulls	- $ZnCl_2$ - KOH - H_3PO_4 - K_2CO_3
Steam-Pyrolysis	One-step	- Olive - Bagasse - Peanut hulls - Grape seeds - Nutshells - Almond shells	–

The thermal decomposition of materials occurs, which produces a fixed carbon mass with closed and tiny pores. In the next step, the activation of carbonized materials where the small pores can be chemically or physically converted into larger pores happens. The carbonization and activation can potentially be carried out in one step through the chemical activation process in which the materials decompose by heat stress with a specific chemical agent (Mohammadi et al., 2021).

The ratio between the chemical agent's mass and the raw material determines the characteristics such as pore size distribution and the activated carbon's surface area. Moreover, parameters such as carbonization temperature, activation time, and thermal rate are critical in specifying the desired activated carbon's overall properties (Lee et al., 2019). It is worth mentioning that raw materials have a decent amount of carbon content and minimized inorganic compositions for the synthesis of activated carbon (Bhatnagar et al., 2015).

1.9 Low-cost adsorbents

Generally, the "low-cost" term refers to an adsorbent that abundantly exists, is less time-consuming to process, minimized cost of operation and is a waste material or by-product manufactured in an industrial site (Amuda et al., 2007). Cost-effective alternatives for activated carbon have attracted more attention due to the high cost of coal-based activated carbons (Abatan et al. (2019)). In terms of the importance of low-cost adsorbents and/or bio-sorbents in water decontamination processes, various review articles have been published, mainly either adsorbate-specific (metals, dyes, phenols, etc.) or adsorbent-specific (Amuda et al., 2007).

According to Figure 1.6 (Singh, 2018), there is a wide variety of materials such as agricultural by-products and residues, industrial wastes, biomass-derived, and natural materials utilized for the decontamination of wastewater and waters. The proper adsorbent, which is low-cost, non-poisonous, easy to regenerate, and accessible, is chosen based on the pollutant concentration, type, productivity, and adsorption capacity (Singh, 2018).

Biomass-derived products such as Aspergillus Tereus (De Gisi et al., 2016) and Rhizopus aarhizus (Bhatnagar and Minocha, 2006) are adsorbents that play an imperative role in eliminating heavy metals and organics in municipal and industrial discharge (Namasivayam and Ranganathan, 1995).

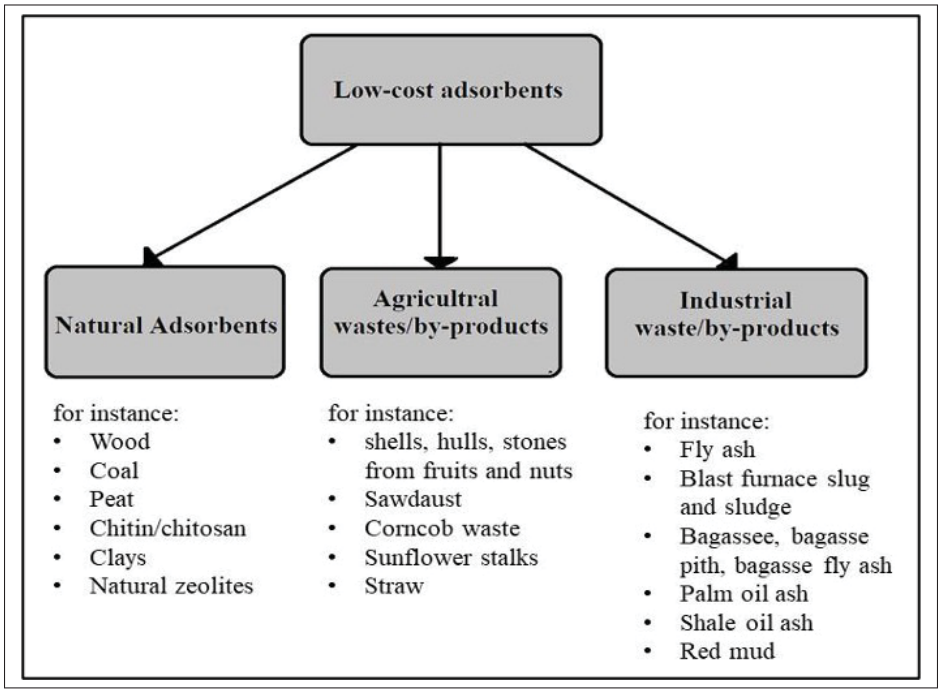

Figure 1.4 An insight into different categories of low-cost adsorbents (taken from Singh, 2018)

1.9.1 Classification of low-cost adsorbents

The classification of activated carbons is multifaceted, encompassing considerations such as the source of the raw material, activation methods employed, pore size distribution, and specialized applications. Understanding these classifications is fundamental to appreciating the nuanced roles that activated carbons play in different contexts. This discussion will explore each classification in detail, shedding light on the unique characteristics that make each type suitable for specific applications.

1.9.2 Natural adsorbents

Chitin, clay, peat moss, wood, zeolite, and coal are known as natural adsorbents, which have been employed to eradicate heavy metal ions, dye composites, and organic compounds in waste and wastewater (Saifuddin M and Kumaran, 2005). Chitin [2-acetamido-2deoxy-glucose-(N-accetylglucan)] is one of the most convenient natural biopolymers in adsorption processes (Singh, 2018). Chitin is originally the principal skeletal component of insects, crustaceans, fungi, algae, and marine invertebrates such as crabs and shrimps (Babel and Kurniawan, 2004; Liu et al., 1994; Rodriguez-Reinoso et al., 1995; Yang and Zall, 1984). Chitosan is a deacetylated polymer extracted from chitin, typically produced through deacetylation with an alkaline solution (Figure 1.5). It can chelate five to six times greater amounts of metal ions than chitin due to the existence of free amino groups that appear after the deacetylation of chitin (Kyzas, 2014).

It is worth mentioning that for a successful sorption process of metal ions through chitosan, active binding sites are easily clustered and tend to convert into gel in aqueous solutions must be available. For this objective, the approachability of metal binding sites must be enhanced through physical support. Furthermore, it has low solubility in low pHs and is defective in commercial utilization (Babel and Kurniawan, 2004).

Another efficient natural adsorbent widely used and broadly available is wood . One of its significant advantages of using wood is that no regeneration is required. Also, we can dispose of it easily through the ignition process (Singh, 2018).

1.9.3 Agricultural wastes

Agricultural wastes are considered the discarded wastes of agricultural residues, fruits, and vegetable peels that have no value in operating and contaminate the environment. However, they can be widely used as low-cost, biodegradable, and economic adsorbents in wastewater treatment to remove several contaminants in aqueous solutions if slight modifications are applied to them (Singh, 2018; Kalpna et al., 2011).

The main components of agricultural waste are lignin and cellulose. Besides, they may also contain polar functional groups of lignin comprised of alcohols, aldehydes, ketones, carboxylic, phenolic, and ether groups competent in binding aquatic contaminants employing various binding processes (Amuda et al., 2007). Various attempts have been made to develop modes of making fruits and vegetable wastes valuable during the recent decade. Agro-industrial wastes are products of great significance, and the recovery of such wastes is of great economic concern (Amuda et al., 2007).

There is a wide variety of biomass agricultural by-products such as rice husk (Hameed et al., 2008), coconut shells, olive wastes (Hjaila et al., 2013; Hamdaoui, 2006), forest industry wastes like sawdust (Zhang et al., 2004), agricultural waste-industry such as oil palm shell (Rafatullah et al., 2010) and banana and orange peel (Shukla et al., 2020). These materials maintain high carbon content and are particularly cost-effective; therefore, they are the best options for producing activated carbon (Lata and Samadder, 2016).

1.9.3.1 Rice Husk

Any plant's base, stem, bark, flower, leaf, fruit skin, husk, shell, or stone can be used to create activated carbon from agricultural wastes. Both woody and non-woody materials can be found in these wastes. Non-woody resources are made up of cellulose, hemicellulose, lignin, lipids, protein, sugar, water, hydrocarbons, starch, and numerous functional groups that may be able to remove contaminants, whereas woody resources are primarily made up of cellulose, hemicellulose, and lignin. Given that it is made from the outer layer of rice grains and mainly consists of silica, cellulose, hemicellulose, and lignin, rice husk is regarded as a non-woody material. Because of their special qualities and potential as a renewable raw material source, non-woody materials like rice husk are frequently used as feedstock to produce activated carbon. Due to its availability, affordability, and possibility for a high adsorption capacity, rice husk is a preferred material to produce activated carbon (Yahya et al., 2015).

Due to their unique composition, non-woody agricultural wastes are favored by researchers for studying the applications of activated carbon, as they can produce better pore structure characteristics compared to woody agricultural wastes. The choice of raw material for activated carbon production is determined (Barroso-Bogeat et al., 2019):

1. High carbon concentration,
2. Low inorganic matter content results in low ash levels,
3. Widely available, ensuring that raw materials are always very affordable,
4. High-density and highly volatile matter,
5. Possibility for activation to continue,
6. Low rate of degradation after storing,
7. Potential to produce an activated carbon with a high percent yield .

One type of affordable material is rice husk. Around 140 million tons of rice husk are produced globally each year (Kalderis et al., 2008). Rice husk is often thrown or burnt in the field, which is harmful to the ecology (Chen et al., 2011). According to reports, rice husks have a high ash content of about 22% and a low calorific value of 3585 kcal kg1. Dry rice husk is composed of 20–25% silica and 70–85% organic matter, including 21.4% lignin, 32.2% cellulose, and 21.3% hemicellulose (Bakar et al., 2016).

Also, there are other metallic impurities present in trace amounts. Like the features of rice husks, rice husk ash's characteristics might change depending on where it is grown. Since it prevents pore growth and results in activated carbon with low mechanical strength and adsorption capacity, the high ash concentration in rice husks is problematic when making it (Yeganeh et al., 2006, enassi et al., 2015).

1.9.3.2 Sugarcane cane bagasse

The Sugar cane bagasse's chemical composition makes it a viable feedstock for a wide range of applications. It often contains high levels of lignin (21%), ashes (5%) and extractive (2%), as well as cellulose (44%) and hemicellulose (28%) (Ajala et al., 2021). Numerous uses for sugarcane bagasse exist, including the creation of paper, wood, and other cellulose-based goods. It is also a typical feedstock for the synthesis of biofuels like ethanol and biogas as well as for the combustion-based production of heat and energy.

Additionally, sugarcane bagasse can be used as a supply of organic matter for soil amendment or as animal feed. Carbon dioxide (CO_2) is not primarily produced by sugarcane bagasse, but it can be added as a physical agent to some processes that are. A fibrous residue called bagasse is created when the sugarcane fibres are crushed to extract the juice. Carbon dioxide is produced when sugarcane bagasse is burned. However, sugarcane bagasse cannot be burned or fermented before being utilized as a physical agent to produce CO_2. As an example, sugarcane bagasse will ferment when used as a feedstock for the generation of biogas, releasing CO_2 and methane. In the same way, burning sugarcane bagasse will result in the production of CO_2 if it is done so to generate heat or energy (Ajala et al., 2021; Gopalakrishnan and Nahan, 1977).

In this work, sugarcane wood is utilized as an activating agent in physical activation. In certain ways, sugarcane is seen as an environmentally favourable fuel source, but it is also connected to several environmental issues. On the positive side, sugarcane can be farmed responsibly and is a renewable resource. It is an excellent fuel source for some applications since it has a high energy density and little moisture. Sugarcane biomass also contributes to a reduction in carbon dioxide emissions since it only releases carbon dioxide that has already been absorbed during growth when it is burned. If the sugarcane is replanted and cultivated once more, this can be regarded as a carbon neutral (Mann, 2016).

The use of sugarcane wood as fuel raises a few significant environmental issues, though. For instance, cultivating sugarcane needs a lot of water and fertilizer, which can lead to soil erosion and water contamination. In addition, the removal of land for the cultivation of sugarcane can

result in deforestation, which can have detrimental effects on the environment by causing wildlife to lose their habitat. Finally, the handling and processing of sugarcane may release toxins and greenhouse gases into the air (El Chami et al., 2020). Figure 1.6 demonstrates the sugarcane bagasse that is being used in this study.

Figure 1.5 Sugarcane bagasse residue selected as a physical agent material

1.9.4 Rice husk-activated carbon

Activated carbon is an adsorbent with a highly developed porosity, a flexible pore composition, extended interparticulate surface area, resistance to heat stress, low acid/base reactivity, and versatility (Goyal, 2005). These characteristics make activated carbon a proper adsorbent to treat comprehensive sorts of organic and inorganic contaminants dissolved in either aqueous or gaseous environments. Therefore, the development of activated carbon (AC) has drawn the attention of researchers in this field since there is a wide variety of treated amorphous carbon-based materials that can be constituted into activated carbon groups (Sawyer, 2003; Zietzschmann et al., 2014). However, one significant defect with operating activated carbon is the need to regenerate the adsorbent's pores after the gas or liquid's adsorption process (Lee et al., 2019).

Activated carbon can be in the form of powder or granular. Because of the regenerability, Granular activated carbon (GAC) is commonly deemed to be more flexible to adapt compared to powdered activated carbon. Due to GACs' adaptability, they control a large portion of the carbon market (Activated Carbon Markets, 1994), especially for raw sugar decolorization (Ahmedna and Rao, 2000).

1.9.5 Carbonization/activation as combined process

As the temperature rises, the carbonization process can be separated into four distinct stages. When the temperature remains below 200°C, the raw material begins to dry. Small amounts of pyroligneous liquids and non-condensable gases are created during the pre-carbonization phase when the temperature rises from 170 to 300°C. The production of charcoal occurs at a temperature of 250 to 300°C as a significant amount of the pyroligneous liquids and tars created during the preceding stage are eliminated. When the temperature hits 300°C and the carbon concentration rises, the diffusion of volatile matter content occurs in the final step (Sánchez-Borrego et al., 2021).

1.9.6 Methodologies to produce low-cost activated carbons

Activated carbon sources are plentiful these days, and they are just growing wider. Precursors to produce activated carbon can be any low-cost material with a high carbon content and low inorganics content. For commercial-grade carbons, powdered activated carbon (PAC) and granular activated carbon (GAC) are the two primary types of activated carbon for water treatment. Surface area values generally range from 500 to 1500 $m^2 \cdot g^{-1}$, with some exceeding 3000 $m^2 \cdot g^{-1}$. They are divided into two sub-categories based on their applications: gas phase and liquid phase, with the former being microporous (pore diameter < 2 nm) in granular form (2.36–0.83 mm, or 8/20 mesh size) and the other one being mesoporous (pore diameter between 2 and 50 nm) in powdered form (0.15–0.04 mm, or 100/325 mesh size)(Saleem et al., 2019) .

Table 1.6 The content analysis of olive-seed waste and char chemical composition (taken from Stavropoulos and Zabaniotou, 2005)

Chemical composition	Raw material (% w/w)	Char
N	1.95	1.35
C	49.7	75.6
H	6.06	0.79
S	0.18	0.00
O	39.0	12.1
Ash	3.00	10.0

Stavropoulos and Zabaniotou, 2005 reported how to produce and characterize activated carbon from olive-seed waste residue. In this article, the activated carbons are produced from olive-seed waste residues through chemical activation by KOH as the activating agent. Samples were generated by activation at 800°C and 900°C for varied times (8 times, depicted in Table 1.7) to investigate the impact of activation time and temperature on the textural qualities of the products. A two-stage procedure was used, with the precursor material being pyrolyzed first, then the char being activated with KOH.

The assessment of the surface area and pore size distribution by N_2 adsorption at 77 K and adsorption of methylene blue from aqueous solutions have been the mainstays of activated carbon characterization. In the process of carbon preparation, the olive-seed waste residue was pulverized and sieved to particle sizes of 125–160 μm, then dried for 24 hours at 900°C. Then, pyrolysis of the olive-seed waste at 800°C for 1 hour in an inert environment (100 cc·min^{-1} N_2) demonstrated in Table 1.6 by w/w on a dry basis (Stavropoulos and Zabaniotou, 2005).

During pyrolysis studies, an average weight loss of 70% was achieved Stavropoulos and Zabaniotou, 2005. Olive kernels are a useful starting material for the generation of activated carbons because they lack sulfur and have a low ash level in the char. Then the char was mixed with KOH in a ratio of 1:4. For remaining KOH removal, carbonized products were chilled and washed in HCl for 1 hour. The acid-washed samples were then washed numerous times with distilled water until they reached a neutral pH. In the drying process, the ultimate carbon products were dried at 110°C for 24 hours. As demonstrated in Table 1.7, the specific surface

properties and porosities of certain carbon samples were determined using N_2 adsorption at 77 K and in liquid-phase adsorption studies, methylene blue (MB) was used as the adsorbate. When the activation time and temperature increase, the BET surface areas of carbons also increase from a minimized value of 1339 $m^2 \cdot g^{-1}$ at 1 hour and 800°C to a maximum of 3049 $m^2 \cdot g^{-1}$ at 4 hours and 900°C (Stavropoulos and Zabaniotou, 2005.

1.9.7 Acid-base leaching of the precursor

It is frequently done to prepare activated carbon from a variety of precursor materials using acid and base leaching. The precursor material is subjected to acid or basic solutions during the process to eliminate impurities, enhance porosity, and produce high-surface-area activated carbon (Tan et al., 2008).

The precursors, specifically the agricultural residue such as rice husk, may be leached either before or following the activation phase. However, the method used to leach the rice husks has an impact on the final product's quality of activated carbon. In terms of specific surface area and micropore volume growth, the leaching sequence carbonization-activation-leaching is more effective than the sequence carbonization-leaching-activation (Muniandy et al., 2014, Petrovic et al., 2022).

In the process of base leaching, SiO_2 is mostly eliminated when rice husks are leached with a base like NaOH because it reacts with NaOH to form sodium silicate (Na_2SiO_3). The created Na_2SiO_3 is easily removed by water-washing because it is soluble in water (Liou and Wu, 2009).

The equation below presents the reaction:

$$2\mathrm{NaOH(s)} + \mathrm{SiO_2}(s) \rightarrow \mathrm{Na_2SiO_3}(s) + \mathrm{H_2}O(l) \tag{1.12}$$

1.9.8 Physical activation by CO_2 emission

An activating agent, such as CO_2, steam, or air, is used to heat a carbon-rich substance, such as wood, coconut shells, or peat, to eliminate any volatile organic chemicals and form a porous structure within the carbon. The carbon's surface area is significantly increased by this porous structure, which makes it very efficient at adsorbing pollutants and impurities from gases and liquids. Due to its advantages for the environment, CO_2 is used more frequently as an activating agent. When compared to conventional activation methods, CO_2 activation produces fewer pollutants and is thought to be a more environmentally friendly strategy. Additionally, the activation process's CO_2 can be recovered and used again, increasing the process' total energy efficiency (Gunawardene et al., 2022).

In general, the creation of previously inaccessible pores, the development of new pores, and lastly the broadening of existing ones are the three stages of the formation of pores by activating gas. The reactions that could occur during activation using various kinds of activating agents are listed below (Yahya et al., 2015).

Carbon dioxide:

$$C + O_2 \rightarrow 2CO \tag{1.13}$$

Steam:

$$\mathrm{C + H_2O \rightarrow H_2 + CO} \tag{1.14}$$

$$\mathrm{CO + H_2O \rightarrow H_2 + CO_2} \tag{1.15}$$

$$\mathrm{C + 2H_2 \rightarrow CH_4} \tag{1.16}$$

Moreover, adsorption onto rice husks has been utilized to help eliminate Cd from wastewater and metals such as Cd (II), Pb (II), Zn (II), Cu (II), Ni (II), and Al (III) from aqueous effluent (Yalçın and Sevinc, 2000). Yalçın and Sevinc, 2000 investigated the production of activated carbon from the rice husk employing $ZnCl_2$ as the chemical agent and other salt solutions/CO_2 activation. In this study, the dried rice husk samples were mixed with various salt solutions concentrations such as $ZnCl_2$ 0-30% (w/w), $FeSO_4.7H_2O$ (30%) (w/w), $FeCl_3.6H_2O$ (30%) (w/w), KCl 30% (w/w), $CaCl_2.2H_2O$, and afterward were placed in a stainless-steel tubular reactor while CO_2 gas passed through the reactor. The salts help to enhance the efficiency of the generated activated carbon as well as $ZnCl_2$.

In the preparation of activated carbon by impregnation with 10% $ZnCl_2$, the specific surface properties were determined through the BET (Brunauer–Emmett–Teller) method, and the highest BET-specific surface area of the final activated carbon was specified to be 480 $m^2 \cdot g^{-1}$. Areas of activated carbon are comparably lower than the one which is impregnated with the $ZnCl_2$. Table 1.7 demonstrates the chemical composition of activated carbon from rice husk which is impregnated with a 10% $ZnCl_2$ solution where the carbon content is higher than other contents and nitrogen is not found in the composition. Also, it is concluded that the surface area and the porosity of the final activated carbon from rice husk are maximized if it is impregnated with a 10% salt solution (Yalçın and Sevinc, 2000).

In the research of Ahmedna and Rao, 2000 two samples of rice straw, rice hulls, and sugarcane bagasse as group 1 with low density and pecan shells as group 2 in the category of agricultural

Table 1.7 Chemical composition of activated carbon from rice husk impregnated with 10% $ZnCl_2$ (taken from Yalçın and Sevinc, 2000)

Chemical composition (% w/w)	C	H	N	Others
Activated carbon prepared from rice husk	64.7	0.59	-	31.4

by-products were prepared to produce GAC (Granular activated carbon). In the process of the production of granular activated carbon utilizing group 1, physical activation was employed and by means of group 2, the chemical activation method was opted to execute the conversion of granular activated carbon and at the last stage, the chemical, physical, surface, and adsorption properties of the produced activated carbons from both groups were compared to two commercial reference carbons. Firstly, sugarcane bagasse, rice hulls, rice straw, and pecan shells as group 1 were milled into 10-20 mesh size and the binders (sugarcane molasses, beet molasses, corn syrup, and coal tar) were prepared for the stage of pyrolysis and the activation Yang et al., 2016.

The product of this mixture is called Briquettes which were pyrolyzed by nitrogen gas at 700°C for 1 hour in an inert atmosphere. Afterwards, the briquettes were crushed and sieved into mesh particle sizes of 12-40. A gas mixture of 13% CO_2 and 87% N_2 was used to activate the granules in a 900°C furnace until a 30% burn-off. After cooling off the products, they were washed with 0.1 N HCl to remove ash particles. The carbon yields for GACs (granular activated carbons) manufactured from group 1 by-products utilizing coal tar, cane molasses, corn syrup, and beet molasses as binders were 47-52%, 25-30%, 24-26%, and 25-31%, respectively. The same procedure was implemented on the pecan shells with various pyrolysis conditions and physical and chemical activation. However, the chemically activated carbons were washed with a soxhlet extractor, and 10 drops of 0.01 M lead acetate were added to it (Chilton et al., 2003b).

Table 1.8 demonstrates the conditions employed for producing activated carbon by pecan shells. As a result of this study and as it is depicted in Figure 1.4, Group 1 by-products produced carbons with a small surface area regardless of the binder used. Chemically activated carbons made from the group 2 by-product, on the other hand, had higher surface areas than the reference carbons.

Table 1.8 Pecan shell-based granular activated carbons production (taken from Chilton et al., 2003b)

Activated Carbon	Pyrolysis Conditions	Activation Type	Activation Condition
PS18	1 h at 700°C under N_2	Physical	2 h at 800°C (CO_2)
PS23	1 h at 700°C under N_2	Physical	6 h at 800°C (CO_2)
PS9	1 h at 700°C under N_2	Physical	8 h at 800°C (CO_2)
PS22	1 h at 700°C under N_2	Physical	4 h at 800°C (CO_2)
PS26	2 h soak in 25% H_3PO_4 under N_2	Chemical	1 h at 450°C (air)
PS24	2 h soak in 50% H_3PO_4 under N_2	Chemical	1 h at 450°C (air)
PS11	2 h soak in 50% H_3PO_4 under N_2	Chemical	1 h at 450°C air, (N_2)
PS10	2 h soak in 50% H_3PO_4 under N_2	Chemical	1 h at 450°C (N_2)

Pecan shells were physically activated to yield granular activated carbons with a reduced surface area.

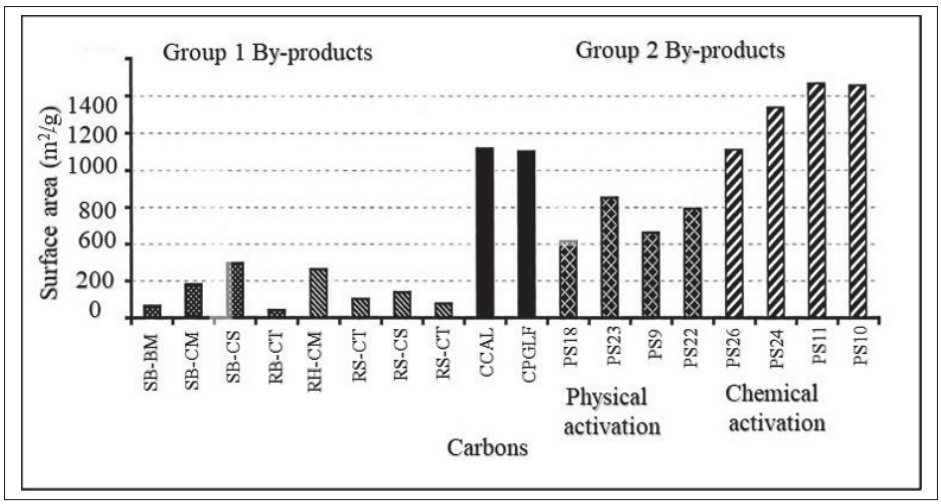

Figure 1.6 Sugarcane Bagasse with Corn Syrup and Coal Tar, respectively; and PS ± Pecan Shells; CCAL and CPGLF are the commercial reference carbons. SB±CS and SB±CT ± Sugarcane Bagasse with Corn Syrup and Coal Tar, respectively; and PS ± Pecan Shells; CCAL and CPGLF are the commercial reference carbons (taken from Ahmedna and Rao, 2000)

Sugarcane bagasse outperformed all other binder types. Rice straw or rice hulls have less capability as a precursor of granular activated carbons with the desirable qualities of sugar-decolorizing carbon than rice straw or rice hulls. Pecan shells, in terms of all the attributes

studied, produced granular activated carbons that were the closest to the reference carbons (Ahmedna and Rao, 2000).

In another study, Sahu et al., 2010 investigated the preparation of activated carbon from tamarind wood collected in West Bengal. $ZnCl_2$ was the activating agent for the precursor. The dry precursor was combined thoroughly with distilled water to yield a concentrated solution containing 10 g of $ZnCl_2$ in 100 mL. For 1 hour, the mixture was mixed at 50°C. After mixing, the slurry was vacuum-dried for 24 hours at 100°C. Under a nitrogen flow rate of 150 $mL \cdot min^{-1}$ STP (Standard temperature and pressure) are conditions that must be maintained for experimental measurements to make comparisons between different data sources. The samples full of chemicals were put in a tubular reactor and heated ($5°C \cdot min^{-1}$) to the final carbonization temperature. N_2 adsorption, X-ray diffraction (XRD), and scanning electron microscopy were used to examine the pore structure of the precursor and modified carbons (SEM). The physio-chemical characteristics of the tamarind wood as the prepared activated carbon resulted in a total pore volume of 1.04 ($cm^2 \cdot g^{-1}$), BET surface area of 132 $m^2 \cdot g^{-1}$, and bulk density of 0.79 $g \cdot mL^{-1}$.

Animal charcoal, also known as bone black, bone char, or abaiser, is a granular product made from the charring of animal bones. Animal bones are a component of the composite that makes up an animal's body. It comprises around 10% carbon, with the rest made up of calcium and magnesium (80%), as well as other inorganic minerals found in bones, and it has a better capacity for extracting coloring pigment from solutions (Yahya et al., 2012). Yahya et al., 2012 utilized chicken, dog, goat, and cow bones to produce adsorbents for the decolorization of palm oil.

In the research by Yahya et al., 2012, firstly, the bone samples were washed and dried before they were placed in various crucibles. The setup was kept in a furnace with a temperature of 400°C for an hour without air. The carbonized bone samples were then crushed, and 200 g of a crushed sample was mixed with 250 mL of 2M Hydrochloric Acid (HCl). Afterward, the mixture was filtered and washed with distilled water and dried in an oven at 800°C for 24 hours. Some specifications of characteristics in activated charcoal, such as ash content, bulk density,

pore volume, and moisture content, were used to characterize the activated carbon. As a result, the most effective adsorbent must have low ash, moisture, and pore volume qualities. The more surface area and carbon content in the activated carbon created, the more effective it is. The activated carbon from cow bones has the best ash content (10.75%), moisture content (3.9%), pore volume (0.3), yield charcoal (96.5%), and fixed carbon values (84.8%).

The objectives of another research by Cechinel and de Souza, 2014 was to assess the efficacy of adsorption of lead onto activated carbon derived from cow bone in aqueous solutions as an alternative to traditional metal uptake techniques. At the first step, the desired particles of 30 mesh were separated before being washed with distilled water and oven-dried—afterward, the activated carbon was acid-washed with 0.2 M HNO_3. Thus, the acquired pH was four and the minimum contact time required for the assays to be performed was six hours. The activated carbon was then filtered, cleaned with distilled water, and put in the oven for 12 hours at 60°C. Finally, the analyzer FAAS (SHIMADZU AA-6300) was employed to examine the liquid phase. The adsorption capacity of 32.1 $mg \cdot g^{-1}$ was obtained in an initial concentration (C_0) of 100 $mg \cdot L^{-1}$ in pH of 4.

Another sort of waste residue left behind after heavy oil processing is petroleum coke (PC). Heavy oil fractions must be converted into light and more desired products by different upgrading technologies to cater to the increasing demands for light oil (Rana et al., 2007). Thermally cracked heavy (residual) oil fractions create light byproducts, which are found in the gas product stream, and a solid product (or PC) with a high content of carbon remains during upgrading pyrolysis. Petroleum coke has a high carbon concentration but low volatile and ash content (Jiang et al., 2008). It can serve as a carbon source for activated carbons. Industrial waste PCs can be converted into cost-effective materials with the appropriate activation procedures.

As Yang et al., 2016 investigated in a study, if petroleum coke is used as a carbon precursor, there is no requirement for a carbonization process to create the porous carbons. This indicates that a treatment process can be skipped when compared to biomass-based KOH-activated carbons, lowering the costs of production. In this study, the aim is to produce a carbonaceous CO_2 sorbent

that is both economical and cost-efficient. Porous nitrogen-doped carbons were generated by integrating ammoxidation with KOH activation using petroleum coke as a precursor. The petroleum coke obtained from a delayed coker was ground and sieved into a particle size of 100-140 mesh (105-150 μm). In the ammoxidation process, the precursor was heated at 350°C for 5 hours in a 10:1 mixture of air and ammonia. The heating rate was 25°C·min^{-1}, and the gas flow rate was 100 mL·min^{-1}.

For the KOH activation process, 2 g of ammoxidation-treated coke was combined in a solution of 4 g KOH at room temperature using a magnetic stirrer for 24 hours. Afterwards, the mixed solution was dried overnight at 120°C in an oven. The samples were activated at 650°C for 2 hours, with a heating rate of 5°C·min^{-1} and a nitrogen flow rate of 400 mL·min^{-1}. The sample generated at a low KOH/precursor ratio (KOH/precursor = 2) and at a mild temperature (650°C) has a CO_2 absorption of 4.57 mmol·g^{-1} at 25°C, which is among the highest for nitrogen-doped porous carbons.

In another study, Jiang et al., 2008 stated that chemical treatment with $HClO_4$ or H_2O_2 and chemical activation with KOH at a constant KOH/coke ratio of 3/1 was used to produce activated carbon from petroleum coke. The petroleum coke was mixed with various concentrations of $HClO_4$ or H_2O_2 before being agitated for 3 hours at 323 K, washed with distilled water, and then dried in an oven for 12 h at 383 K. At a mass ratio of 1:3, the original PC (petroleum coke) or modified sample was physically mixed with KOH. The mixture is heat-treated in a furnace through a flow of nitrogen with a flow rate of 200 mL·min^{-1} from room temperature to 673 K and held at the same temperature of 673 K for 1 hour. For the final activation, the heating rate of 6 K·min^{-1} was used to the final temperature of 1073 K kept for 1 hour. The same coke was activated for 1 hour at 1073 K with KOH (KOH/coke = 4 by weight) under N_2 flow. Prior to activation, chemical treatment significantly improved the BET surface area and total pore volume of the activated carbon. Chemically activated modified petroleum coke-based activated carbon had a larger specific surface area (2336 m^2·g^{-1}) and a higher iodine adsorption value (1998 mg·g^{-1}).

Based on Table 1.9, in research, Aygün et al., 2003, the utilization of almond shell, hazelnut shell, and walnut shell as raw materials for the synthesis of granular activated carbon (GAC) was studied. Physical (attrition, bulk density), chemical (elemental composition, percent weight loss), surface (surface area, surface chemistry), and adsorption properties of GACs were assessed (iodine number, phenol, and methylene blue adsorption). It was resulted that, the methylene blue adsorption capacities of activated carbons made from hazelnut and walnut shells were affected by pyrolysis temperature and $ZnCl_2$ activation time. The sustainability order of the raw materials for granular activated production are hazelnut shell > walnut shell > almond shell.

Also, in another study, Wu et al., 2010, at 30°C, researchers have investigated the adsorption of two commercial dyes (Acid blue 25 and Basic red 22) from water on activated carbons. The carbons were made from bagasse and activated by steam with varied degrees of burn-off by adjusting the temperature between 750°C and 840°C. After grinding in a mill, the carbons were washed and dried. The bagasse-based carbons have pore sizes that were primarily < 2 nm (micropore), with a peak of approximately 4 nm (mesopore). Furthermore, when the extent of burn-off rose from 80.6 to 91.3wt%, the volume fraction of meso/macropores increased from 22.3 to 31.1%. As can be observed, three types of characterizations to produce activated carbon by utilizing bagasse have been mentioned.

Malik, 2003 examined that for the elimination of Acid Yellow 36, activated carbons made from mahogany sawdust and rice husk were used. The findings showed that a pH of 3 is optimal for acid dye adsorption. Sawdust carbon and rice husk carbon had adsorption capacities of 183 mg· g^{-1} and 86.9 mg· g^{-1} of adsorbent, respectively.

Rhodamine-B (RhB) adsorption on treated rice husk-based activated carbon was also studied (Ding et al., 2014). The rice husk was treated with phosphoric acid (50.0 wt.%) in a 1:4 mass ratio, then heated to 500° for 1 hour, and the final mixture was processed in various ways. Rice husk was washed with distilled water until neutral pH in the first mode, which resulted in the synthesis of an adsorbent known as P-AC.

In the second stage, the rice was washed in hot distilled water (95°C) until the pH was neutral, and the solid product was designated P95-AC. Finally, the solid product was rinsed with distilled water until it reached a neutral pH and combined with a 3.00 wt.% potassium hydroxide solution in the third stage.

CHAPTER 2

MATERIAL AND METHODS

The experimental setup and sample techniques are covered in this chapter. This chapter also covers the equipment and chemicals required for the preparation of the materials and experimental activities. To illustrate the entire experiment and make the entire process easier to follow, a process schematic is also included.

Rice husk and sugarcane bagasse, two main agricultural waste products that were used in the present study as low-cost, natural, and secure adsorbents, were bought from nearby local stores in Montreal, Québec. After the adsorbents and adsorbate solutions were prepared, a variety of experimental setups were used for the batch experiments which later are utilized to perform isotherm and kinetics studies.

2.1 Instruments and chemicals

Fisher Scientific is the source of all chemicals used in this study for different processes such as determining the iodine number of the adsorbent and the batch experiments for examining the isotherms and kinetics pertained to the optimum adsorbent. The surface properties and roughness of the adsorbents were studied using scanning electron microscopy (Hitachi SU-8230 SEM). For the pH neutralization process, sodium hydroxide (0.1 mol$\cdot$ L^{-1}) and hydrochloric acid (0.1 mol$\cdot L^{-1}$) solutions were employed in the experiments. Shredder Retsch SM 300 is utilized to reduce the particle size of the rice husk to 2.0 mm or 500 μm to provide a better surface area for the pores to develop. This equipment is utilized to sieve the washed rice husk which generates a powdered-size rice husk for activated carbon production with better physical characteristics.

2.2 Adsorbate sample

In this study, a single variety of rice husks from a local shop is utilized as the low-cost adsorbent of agricultural materials. The raw rice husk is utilized to produce adsorbents in their natural

forms. In the preparation process, the raw rice husk is primarily washed with distilled water and tap water several times to eliminate the dirt and impurities from the material. They are put into the oven at 105°C for 24 h before they are put into the desiccator to avoid further absorption of moisture. Prepared rice husk is stored to be employed as the precursor for the synthesis of activated carbon. Additionally, it is ground and sieved until it reaches the appropriate particle size before the carbonization/activation process.

2.3 Char yield percentage

The char yield of every sample is also calculated after the activation process occurs. The equation is shown as follows:

$$\text{Activation Yield (\%)} = \frac{\text{Final weight of activated carbon after activation (g)}}{\text{Initial weight of raw rice husk (g)}} \times 100 \qquad (2.1)$$

2.4 Synthesis schematic

In the presented Figure 2.2, a comprehensive overview of the entire procedure is depicted. It illustrates the sequential steps involved in sample preparation, encompassing the generation of the precursor through a series of acid/base leaching steps, followed by the combined carbonization and activation process. Finally, the schematic encapsulates the examination of the characterized precursor in the concluding stage.

2.5 Acid and base leaching for activated carbon preparation

Most of the remaining metallic impurities in rice husks are removed by acid leaching, which further prevents the restriction of pore growth. Metals dissolve in acid, causing the elimination of metallic contaminants from rice husks by acid-leaching, and are afterward eliminated by washing the rice husk samples with distilled water. Acid leaching is a crucial stage in the creation

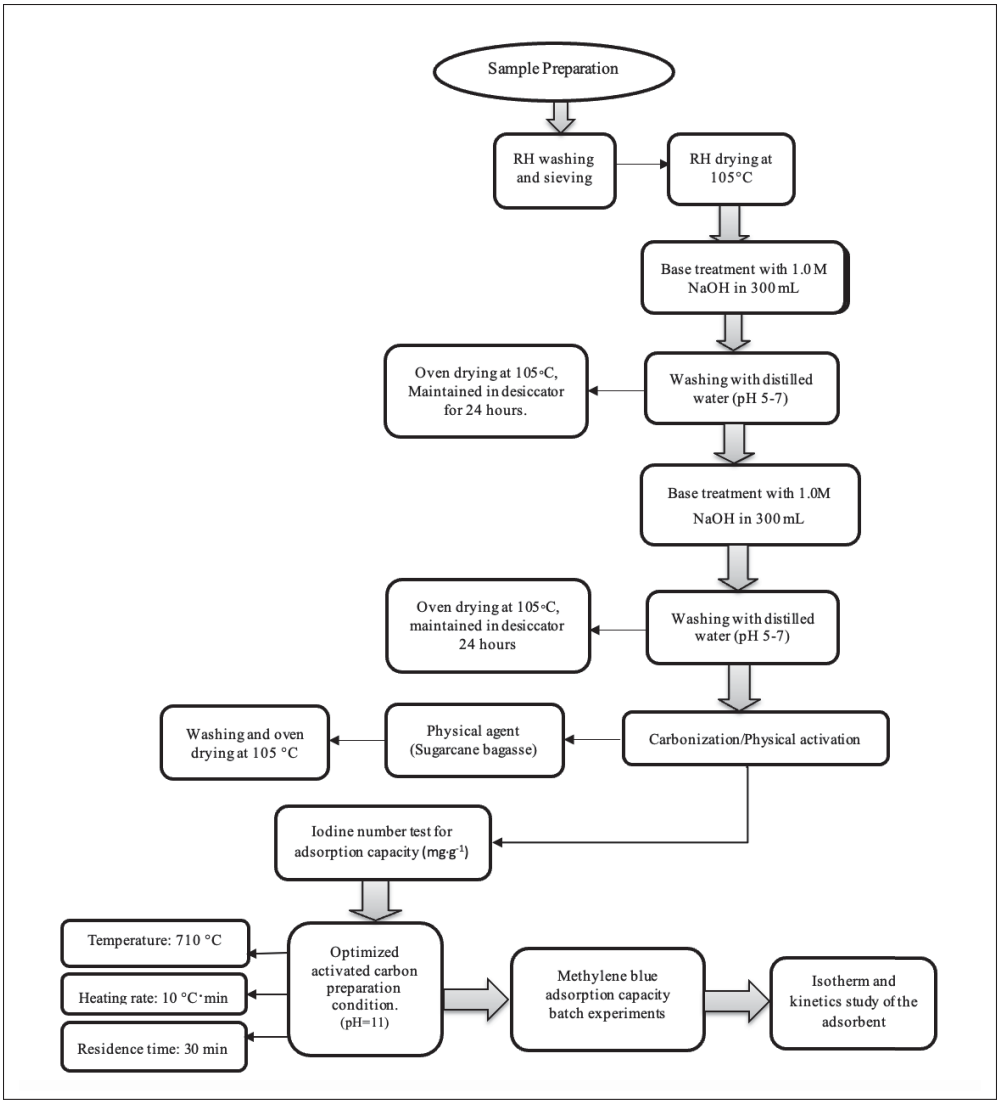

Figure 2.1 A schematic of the experimental phase

of activated carbon because it develops a highly porous structure and adds functional groups that increase the material's ability to absorb (Muniandy et al., 2014)

During the acid-base leaching step, approximately 15 g of washed and sieved rice husk was weighed and then treated with 300 mL of 1.0 M HNO_3 and stirred for various durations. Then the sample was rinsed with distilled water several times to remove the metallic impurities until it reached a neutral pH of 5-7 and the acid content was removed. The oven drying at 105°C for 24

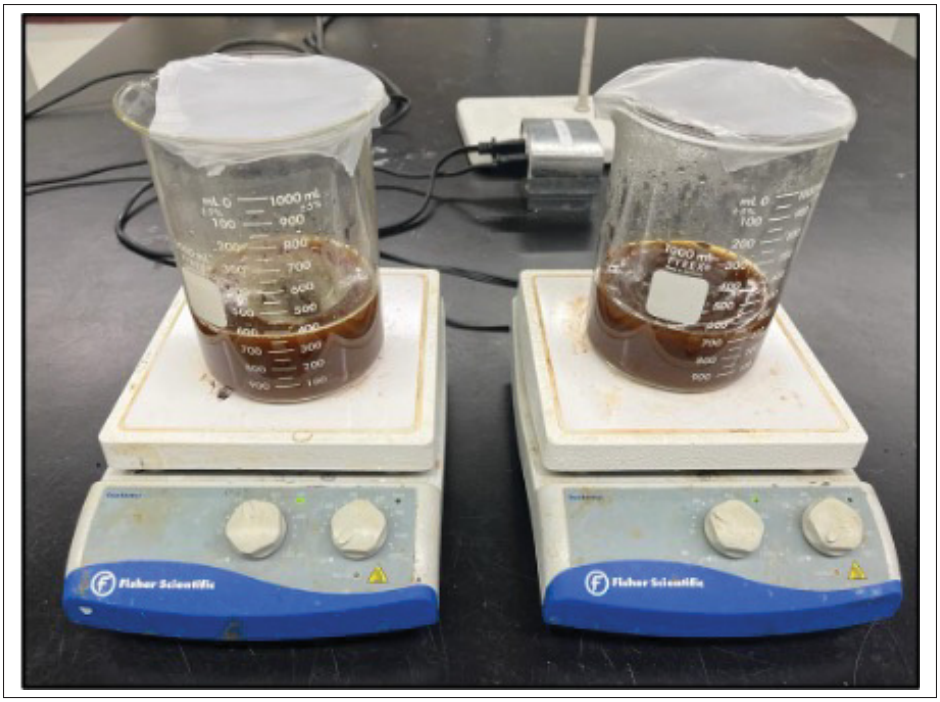

Figure 2.2 Acid-base leaching process of activated carbon before activation process

h is the next step of the process. To remove the silica content of the precursor, the acid-treated precursor is stirred with 300 mL of 1.0 M NaOH for various durations (Muniandy et al., 2014).

The acid-base leached precursor was rinsed with distilled water several times and then it is put in the oven at 105°C for 24 hours to be dried out and stored in the desiccator to avoid moisture. At this stage, the samples are prepared and ready to be used as the precursors for the activation process in which various variables are being examined. In the first trials, the initial weight of the precursor is considered a variable, and the duration time of acid-base leaching, activation time, and temperature are constant.

2.6 Carbonization/activation process with two crucible method

The various processes used to prepare activated carbon are intended to identify the most effective method for manufacturing high-quality activated carbon. Another low-cost material that is utilized in this research is sugarcane bagasse which is used as the physical agent in this procedure.

The sugarcane bagasse is also washed thoroughly several times to remove the impurities and is put in the desiccator to be used as the physical agent for the adsorbent production.

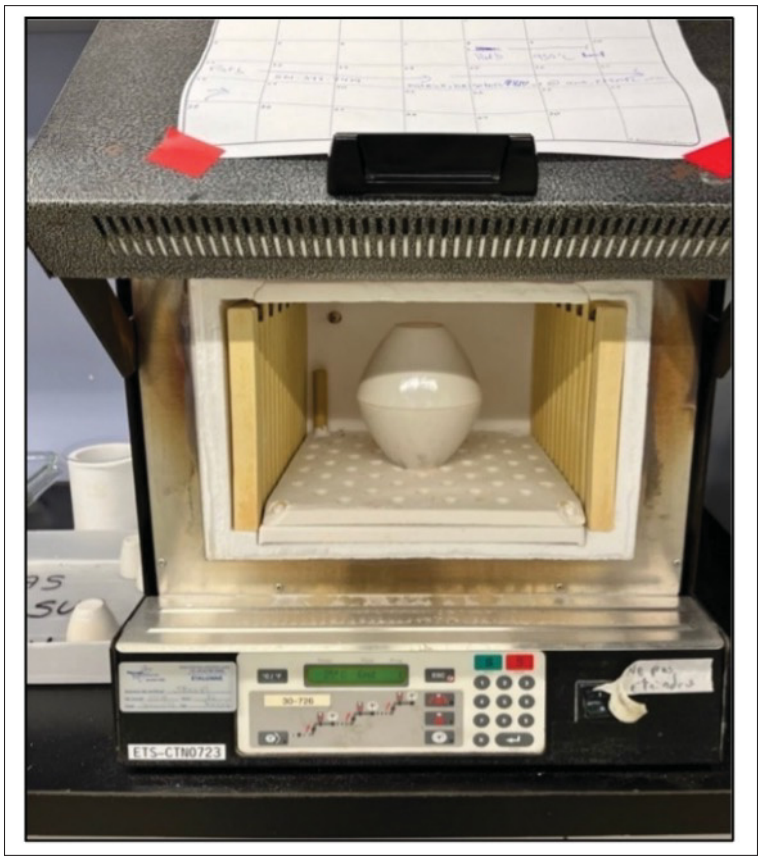

Figure 2.3 Carbonization/activation process

One of the most crucial components of this setup is to reduce the technical requirements and develop a more economical and environmentally friendly way to produce activated carbon. Normally, inert media (the use of N_2, and argon gas) is typically utilized in the production procedure. However, under current local conditions, it is quite difficult to prepare the internal environment for activated carbon. The method that was applied in this research is called the double crucible method which is inspired by Ahiduzzaman and Sadrul Islam, 2016. Figure 2.5 demonstrates the rice husk-activated carbon after the carbonization/activation process.

The prepared rice husk is put into a small and round porcelain crucible and then it is put in a bigger porcelain crucible in which the empty area in this crucible is filled with sugarcane bagasse.

Another big porcelain crucible is used as a lid to minimize the entrance of oxygen into the setup. Firstly, the exhaustion of the sugarcane bagasse provides an amount of CO_2 gas that can be used as a physical agent to help manufacture a better adsorbent surface. Secondly, it is important to notice that avoiding the entrance of air is not utterly possible because the crucibles can expand while being heated and cooled down. Figure 2.4 demonstrates the actual two-crucible method setup to produce activated carbon from rice husk. Once the setup is prepared, it is placed inside the oven to undergo carbonization/activation. The specific alterations in the variables that drive this process are comprehensively detailed in the sampling procedure.

Iodine adsorption testing is the initial step in the evaluation of the activated carbon. Finding the ideal mixture of activation parameters (precursor, temperature, activation agent, and degree of heat treatment) and preparation parameters (acid-base leaching duration, the initial weight of precursor) to produce the optimum result from rice husk is one of the key goals of this study. To accomplish the goal, several actions and procedures are sequentially carried out.

a) Precursor before carbonization/activation

b) Precursor after carbonization/activation

Figure 2.4 The preparation of rice husk activated carbon

2.7 Iodine Number Methodology

Iodine Number Test for adsorption following the procedure outlined in ASTM D4607-94. The iodine number is then calculated. The milligrams of iodine adsorbed by 1.0 g of carbon at a filtrate iodine concentration of 0.02 N is known as the "iodine number" (0.02 mol·L^{-1}). A three-point isotherm is the foundation of this approach. Under the circumstances, three different weights of activated carbon are used to treat a conventional iodine solution. The activated carbon sample will be treated with 10.0 mL of 5% HCl for the experiment. This combination boils for 30 seconds before cooling. Then, the mixture is quickly combined with 100.0 mL of 0.1 N (0.1 mol·L^{-1}) iodine solution, and it is agitated for 30 s.

The resultant solution is filtered, and using starch as an indicator, 50 mL of the filtrate is titrated with 0.1 N (0.1 mol·L^{-1}) sodium thiosulfate. Using logarithmic axes, the quantity of iodine absorbed per gram of carbon (X/M) is plotted against the amount of iodine present in the filtrate (C). The entire operation should be repeated using alternative carbon masses for each isotherm point if the residual iodine concentration (C) does not fall within the range of 0.008 to 0.04 N (0.008 to 0.04 mol·L^{-1}) after being removed from the sample. For the three points, a regression with the least squares fitting is used.

The equations below are used to determine the X/M and C values, respectively:

$$\frac{X}{M} = \frac{(N_1 \times 126.93 \times V_1) - \left(\frac{V_1 + V_{HCl}}{V_F}\right) \times (N_{Na_2S_2O_3} \times 126.93 \times V_{Na_2S_2O_3})}{M_c} \tag{2.2}$$

$$C = (N_{Na_2S_2O_3} \times V_{Na_2S_2O_3}) \tag{2.3}$$

Where:

$\frac{X}{M}$ = iodine adsorbed per gram of carbon, ($mg \cdot g^{-1}$),

X = Mass of iodine (g),

M = Mass of substance being tested (g),

N_1 = sodium thiosulfate solution normality (N),

$V_{Na_2S_2O_3}$ = consumed volume of sodium thiosulfate solution (mL),

M_C = mass of the precursor (g),

V_i = added volume of iodine solution (mL),

V_f = filtrate volume utilized in titration (mL),

HCL = added volume of 5% HCL (mL).

2.8 Kinetics and isotherm study

In a 1000 mL volumetric flask, 1 g of methylene blue powder was dissolved in a small amount of distilled water to create absorbency. To make up the difference, more distilled water was added. The stock solution, which had a concentration of 1000 $mg \cdot L^{-1}$, was then vigorously agitated for five minutes to make a totally dissolved and homogenous solution. By following dilution, various concentrations were created. To analyze the impacts of pH solution, dye concentration, contact time, and adsorbent dose, batch adsorption was used. The optimal value of pH is determined by examining the highest rate of methylene blue removal in the filtered solutions.

The optimum condition for adsorbent dosage is selected to investigate the effect of pH on the adsorption process. HCL (0.5M) and NaOH (0.5M) are used to standardize the solutions to various pH. The absorbance is examined, and the optimum condition which is discussed in results chapter. After experimenting with various preset time intervals, the equilibrium contact times were established for each adsorbent.

According to the following equation, the lead ions' adsorption capabilities were determined:

$$q_e = \frac{C_e - C_i}{M \cdot V} \tag{2.4}$$

Where:

C_i = initial concentration of the methylene blue ($mg \cdot L^{-1}$),

C_e = equilibrium concentration of the methylene blue ($mg \cdot L^{-1}$),

M = initial adsorbent dosage (g),

V = volume of the adsorbate (L),

q_e = adsorption capacity of the adsorbent ($mg \cdot g^{-1}$).

Also, the percentage of methylene blue (MB) removal for each experiment as it is shown in the following figure 2.7 is calculated as mentioned below:

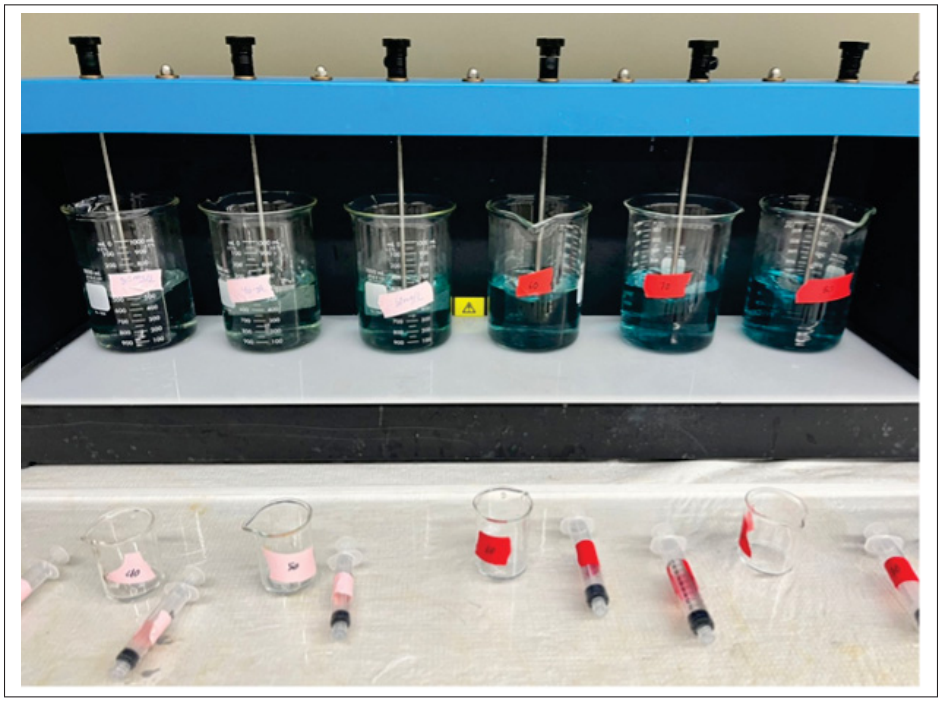

Figure 2.5 Kinetics and isotherm batch experiments

$$\text{Methylene Blue removal (\%)} = \left[\left(\frac{C_i - C_e}{C_i}\right) \times 100\right] \tag{2.5}$$

A calibration curve is generated to establish a connection between each absorbance (y) and its corresponding concentration is as follows:

$$\text{Concentration (mg·L}^{-1}\text{)} = \frac{y - 0.0122}{0.0175}$$

CHAPTER 3

RESULTS

In this section, the obtained results will be presented and analyzed, focusing on the optimization of activated carbon production for iodine adsorption. The investigation explored various parameters, including activation temperature, acid-base leaching duration, and the initial weights of precursor materials. These factors were systematically examined to determine their influence on the iodine adsorption capacity of the resulting activated carbon. The aim was to identify the optimal conditions that would yield activated carbon with enhanced iodine adsorption properties.

3.1 Finding the optimal condition for RH-activated carbon production

As detailed in the preceding chapter on materials and methods, a series of procedures were executed to generate the RH precursor. The results of each step are presented in diverse tables. These tables demonstrate the assessment of various factors, including acid/base leaching, the initial weight of RH, the initial weight of the physical agent, and heating rate as well as temperature and contact time. The iodine number of each produced precursor is determined, and the most optimized value is selected to produce RH-activated carbon with the highest adsorption capacity. Additionally, the precursor undergoes a characterization process. All the experiments are performed at room temperature (25°C).

3.1.1 The optimum selection of initial rice husk weight

In Table 3.1, the initial focus of the first series of experiments is on assessing the influence of varying amounts of rice husk or RH (5 g to 15 g) in a carbonization/activation process. Throughout these experiments, other factors such as activation time, temperature, acid/base leaching duration, and the weight of sugarcane bagasse (SC) are kept constant. The tests throughout this experiment and the following experiments are done 3 times to make sure of each attained values.

Table 3.1 Impact of rice husk weight on the adsorption capacity

RH_i (g)	**Char Yield (%)**	**Time (min)**	**Temp. (°C)**	**SC (g)**	**Leaching (hour)**	**Heating Rate (°C·min^{-1})**	**Iodine Number (mg·g^{-1})**
5.00	30.8	30	630	10	6	10	681
7.50	21.3	30	630	10	6	10	811
10.0	34.1	30	630	10	6	10	830
12.5	19.2	30	630	10	6	10	781
15.0	7.73	30	630	10	6	10	758

Notably, when opting for 10 g of rice husk, employing conditions of 630°C for 30 minutes with a heating rate of 100°C·min^{-1}, alongside a constant sugarcane bagasse weight of 10 g and a 6-hour acid-base leaching procedure, the iodine number registers at 830 mg·g^{-1}, and the char yield attains 34.1%. This outcome indicates a superior adsorption capacity compared to alternative conditions, prompting the selection of these specific conditions for further investigation in the subsequent set of experiments.

3.1.2 The optimum selection of physical agent (sugarcane bagasse) weight

In Table 3.2, the subsequent phase of experiments involves focusing on the optimal weight of rice husk (RH) established in the previous step. In this stage, the variable under consideration is the weight of sugarcane bagasse (SC), while the other parameters are maintained at constant values. A range of 5 g to 15 g of SC is selected as the physical agent for the carbonization/activation process, conducted at 630°C for 30 minutes with a heating rate of 10°C·min^{-1}.

Table 3.2 Impact of physical agent weight on the adsorption capacity

SC (g)	**Char Yield (%)**	**Time (min)**	**Temp. (°C)**	**RH_i (g)**	**Leaching (hour)**	**Heating Rate (°C·min^{-1})**	**Iodine Number (mg·g^{-1})**
5.00	26.0	30	630	10	6	10	793
7.50	18.0	30	630	10	6	10	811
10.0	17.2	30	630	10	6	10	830
12.5	17.0	30	630	10	6	10	781
15.0	25.9	30	630	10	6	10	759

The chemical procedure involving acid-base leaching persists for 6 hours. Ultimately, the optimal condition, identified as 10 g of sugarcane bagasse, is determined based on achieving an iodine number of 830 $mg \cdot g^{-1}$ and a char yield of 17.0%. This condition exhibits the highest adsorption capacity compared to others tested in this experiment.

3.1.3 The optimum selection of acid-base leaching duration

In Table 3.3, the subsequent phase of experimentation involves fixing two parameters at 10 g each for both rice husk (RH) and sugarcane bagasse (SC) as the physical agent. The focus now shifts to examining the impact of varying acid/base leaching durations, specifically at intervals of 1, 2, 4, 6, 12, and 24 hours.

Table 3.3 Impact of acid-base leaching duration on the adsorption capacity

Leaching (hour)	Char Yield (%)	Time (min)	Temp. (°C)	RH_i (g)	SC (g)	Heating Rate ($°C \cdot min^{-1}$)	Iodine Number ($mg \cdot g^{-1}$)
1	26.1	30	630	10	10	10	799
2	25.2	30	630	10	10	10	814
4	30.0	30	630	10	10	10	603
6	26.4	30	630	10	10	10	650
12	23.2	30	630	10	10	10	758
24	25.8	30	630	10	10	10	616

Throughout this investigation, the remaining parameters remain constant at 630°C for 30 minutes with a heating rate of $10°C \cdot min^{-1}$. Ultimately, the optimal condition (2 hours) is determined, characterized by an iodine number of 814 $mg \cdot g^{-1}$ and a char yield of 25.2%. This condition showcases the highest adsorption capacity compared to the other tested durations.

3.1.4 The optimum selection of activation temperature

In Table 3.4, this series of experiments focuses on determining the optimal activation temperature. The investigation spans temperatures ranging from 590°C to 790°C while maintaining constant values for other parameters, including a 2-hour leaching period, a 10 g weight for both the precursor (RH) and the physical agent (SC), and a heating rate of $10°C \cdot min^{-1}$.

Table 3.4 Impact of activation temperature on the adsorption capacity

Temp. (°C)	Char Yield (%)	Leaching (hour)	Time (min)	RH_i (g)	SC (g)	Heating Rate (°C·min^{-1})	Iodine Number (mg·g^{-1})
590	32.1	2	30	10	10	10	634
630	31.4	2	30	10	10	10	780
670	31.1	2	30	10	10	10	796
710	30.5	2	30	10	10	10	836
750	28.0	2	30	10	10	10	709
790	25.1	2	30	10	10	10	696

The ideal temperature is identified as 710°C, where the iodine number reaches 736 mg·g^{-1}, and the char yield reaches 30.5% which shows the highest adsorption capacity among the other acquired data.

3.1.5 The optimum selection of heating rate

In Table 3.5, in the final series of experiments, we systematically explored and optimized variables such as the initial weights of rice husk (RH) and sugarcane bagasse (SC), acid/base leaching duration, and activation temperature. In this phase, the focus shifts to examining the heating rate, ranging from 5 to 20°C·min^{-1}, while keeping other parameters constant.

Table 3.5 Impact of heating rate on the adsorption capacity

Heating Rate (°C·min^{-1})	Char Yield (%)	Leaching (hour)	Temperature (°C)	RH_i (g)	SC (g)	Time min	Iodine Number (mg·g^{-1})
5.00	34.0	2	710	10	10	30	696
7.50	33.2	2	710	10	10	30	690
10.0	31.5	2	710	10	10	30	721
12.5	31.2	2	710	10	10	30	685
15.0	31.2	2	710	10	10	30	669
17.5	30.8	2	710	10	10	30	665
20.0	23.0	2	710	10	10	30	650

The constants include a 2-hour leaching period, an activation temperature of 710°C, and initial weights of 10 g for both activated carbon and sugarcane bagasse, with an activation time of 30 minutes. The optimal condition, characterized by the highest adsorption capacity, is identified

when the heating rate is set at 10°C·min^{-1}, resulting in an iodine number of 721 mg·g^{-1} and a char yield of 31.5%.

3.2 Adsorbent dosage impact

To assess the adsorption capacity of the adsorbents in dye removal tests, six distinct dosages of the prepared activated carbon (ranging from 0.2 g to 0.7 g) are utilized and labelled as AC1, AC4, AC2, AC5, AC3, and AC6 respectively. These adsorbents are introduced into 500 mL conical flasks containing methylene blue (MB) with a concentration of 50 mg·L^{-1} as the adsorbate. The flasks undergo stirring using a Jar test device set at a constant speed of 150 rpm with a constant pH of 11 for varying time intervals (45 minutes – 60 minutes) until equilibrium is attained.

The experiment involves a systematic examination of varying quantities of activated carbon, revealing a consistent decrease in absorbance over the 72-hour duration. This decline signifies the progressive absorption of methylene blue by the activated carbon. Notably, all samples reach equilibrium between 2 to 6 hours, indicating saturation, wherein the activated carbon can no longer adsorb additional methylene blue. The observed convergence in absorbance at this point serves as a crucial marker for the saturation phenomenon.

These findings contribute valuable insights into absorption kinetics and the capacity of rice husk-activated carbon. The graphical representation of absorbance against time (in hours) for different quantities of activated carbon underscores the optimal dosage for efficient methylene blue removal. This comprehensive analysis enhances our understanding of the dynamic adsorption behaviour of RH-activated carbon and informs optimal application strategies for dye removal processes.

There will be an increase in the dosage of activated carbon (0.7 g) correlates with a decreased time required to attain equilibrium. This equilibrium state represents a constant condition wherein no further adsorbate can be removed, and the system stabilizes. It can be concluded that, As the dosage rises, more active sites become accessible for adsorption, allowing the activated carbon to effectively capture and retain impurities from the substance being treated.

3.3 pH impact

Figure 3.1 illustrates how pH affects the extent to which rice husk-activated carbon-based adsorption operates to remove Methylene blue. Using a constant mass of 0.3 g of the generated activated carbon, this study investigates the effects of different pH values on its adsorption capacity. After doing six different sets of trials at a constant concentration of 50 $mg{\cdot}L^{-1}$, a pattern becomes apparent: when the dye solution's initial pH rises from 3.00 to 11.0, the percentage of dye removal increases in tandem. The pH environment plays a crucial role in the effectiveness of the adsorption process, and the type of adsorbent used will determine the ideal pH range for removal. Interestingly, the trend gets stronger in this case as the solution leans more toward an alkaline environment. Increased pH levels could result in a rise in the amount of negative charges on the surface of activated carbon, which may enable electrostatic interactions with positively charged substances such as Methylene Blue. In alkaline conditions, this will result in an increase in adsorption capacity and efficiency (Kuang et al., 2020). A notable 94.1% removal rate at pH 11.0 indicates a significant improvement in dye removal efficiency.

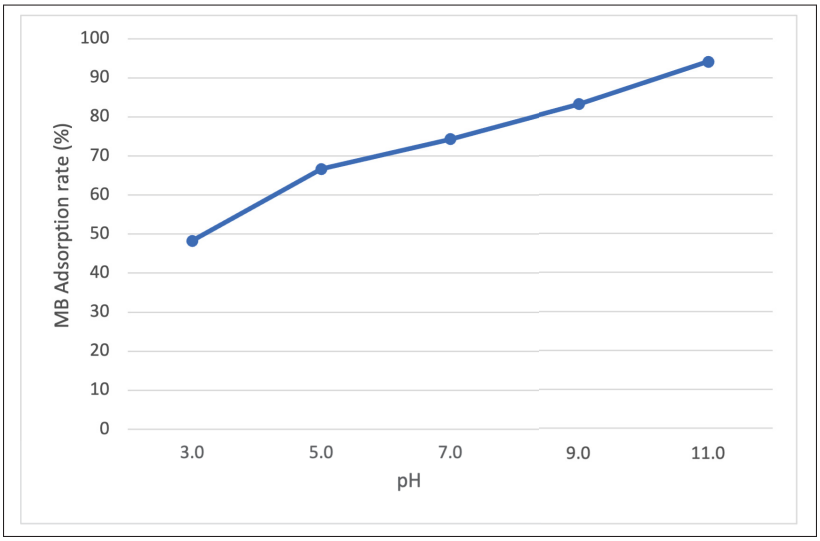

Figure 3.1 The influence of various pH levels on adsorption rate for Methylene blue adsorption using 0.3 g of rice husk-activated carbon at a concentration of 50 $mg{\cdot}L^{-1}$ at 25°C

Adjusting the pH environment for best results is important, as seen by the positive link between higher pH levels and improved dye removal—which is especially evident in alkaline settings. To optimize the use of rice husk-activated carbon in wastewater treatment applications, environmental variables can be wisely adjusted. This perceptive investigation illuminates the complex relationship between pH and adsorption efficacy.

3.4 Initial concentration (C_0) impact on the removal percentage

This study looked carefully at the impact of initial concentration (C_0) on the activated carbon based on rice husk's adsorption performance for the removal of methylene blue (MB). With different initial MB concentrations (ranging from 30 $mg{\cdot}L^{-1}$ to 70 $mg{\cdot}L^{-1}$) at an optimum pH of 11, the experimental setup entailed varied contact times from 5 minutes to 360 minutes at 25°C. Figure 3.2, which plots the percentage removal of MB against various contact durations, provides a clear illustration of the effect of contact time on MB adsorption.

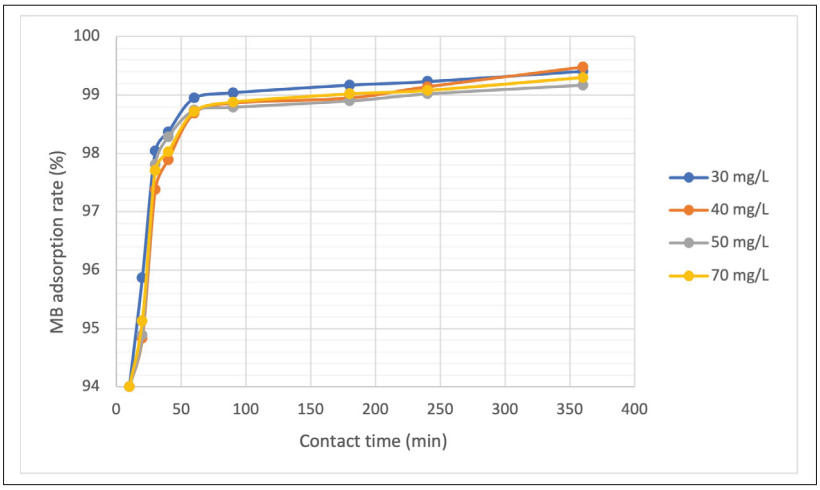

Figure 3.2 The impact of initial concentration (C_0) of Methylene blue on the removal efficiency showcasing various concentrations (pH=11, 0.3 g of rice husk activated carbon, 25°C, contact time = 72 hours)

As you can see in figure 3.2, the data clearly shows that the removal efficiency shows a trend that increases with initial concentration (C_0). As depicted in the figure, the sample containing 70

mg·L^{-1} exhibits a more substantial reduction in Methylene blue (Mb) percentage. The fast uptake of MB during the first 0 minutes to 50 minutes of the adsorption process is a sign that the active binding sites on the activated carbon derived from rice husk are rapidly saturated. After a longer contact period, the removal efficiency reaches a plateau and then keeps increasing. This plateau emphasizes the significance that initial concentration plays in establishing optimal adsorption capacity. Equilibrium is reached when the rate of adsorption equals the rate of desorption.

3.5 Effect of contact time and adsorbent dosage

Figure 3.11 presented provides significant insights into the dynamics of methylene blue adsorption employing rice husk-activated carbon throughout little more than 400 minutes. The plot shows the differences between six initial adsorbent dosages (0.2, 0.3, 0.4, 0.5, 0.6, 0.7 g) in 50 mg·L^{-1}. A different colour represents each dosage.

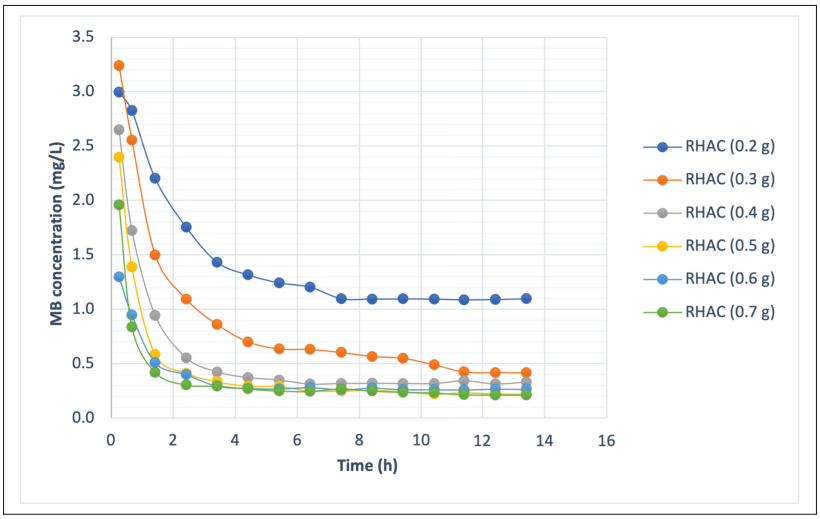

Figure 3.3 The study of methylene blue concentration variances versus time with various rice husk activated carbon dosages (pH = 11, Contact time 12 hours, agitation speed at 150 rpm, 25°C,)

During the first 100 minutes, there is a noticeable rapid decrease in concentration at all concentrations, indicating a successful and quick adsorption process as the adsorbent dosage increases. At each concentration level, the rate of concentration reduction then gradually slows

down, and the readings eventually plateau at 200 minutes. This implies that the RH-activated carbon has successfully absorbed and saturated with methylene blue molecules, indicating a possible state of equilibrium or the end of the adsorption process.

The data points for each concentration level stay mostly unchanged after the equilibrium point, showing little to no change over time. This concentration plateau suggests that either the process affecting concentration has slowed down significantly or is no longer actively eliminating methylene blue. The uniform adsorption process, which may involve the saturation of accessible binding sites on the RH-activated carbon, is implied by the constant behaviour across concentrations. This behaviour is consistent with a situation in which a chemical reaction achieves its endpoint or reaches saturation, demonstrating the effectiveness and consistency of RH-activated carbon in adsorbing methylene blue for the duration of the experiment.

3.6 Removal of Methylene blue for different adsorbent dosages

Different adsorbent amounts were evaluated in the given dataset to see how they affected the percentage of dye removal. The batch adsorption was studied in the condition where 6 different initial weights of RH-activated carbon from 0.2 g to 0.7 g undergoes stirring using a Jar test device set at a constant speed of 150 rpm with a constant pH at 11 for varying time intervals (45 minutes – 60 minutes) until equilibrium is attained.

According to Figure 3.4, the percentage of dye removed at a dosage of 0.2 g of adsorbent was recorded at 70.3%. Significant improvements in removal efficiency were obtained with subsequent dosage increases. To be more precise, the elimination percentage increased to 88.7% at 0.3 g and then to 90.6% at 0.4 g. There was a higher clearance percentage of 93.9% at a dosage of 0.5 g, suggesting a favorable relationship between dosage and removal efficiency. Remarkably, at 0.6 g, the clearance percentage showed a slight decrease, ultimately resting at 92.7%. At 0.7 g, the trend of ascent resumed, resulting in a removal percentage of 94.1%. The dataset suggests the presence of an optimal adsorbent dosage for maximizing dye removal efficiency, as indicated

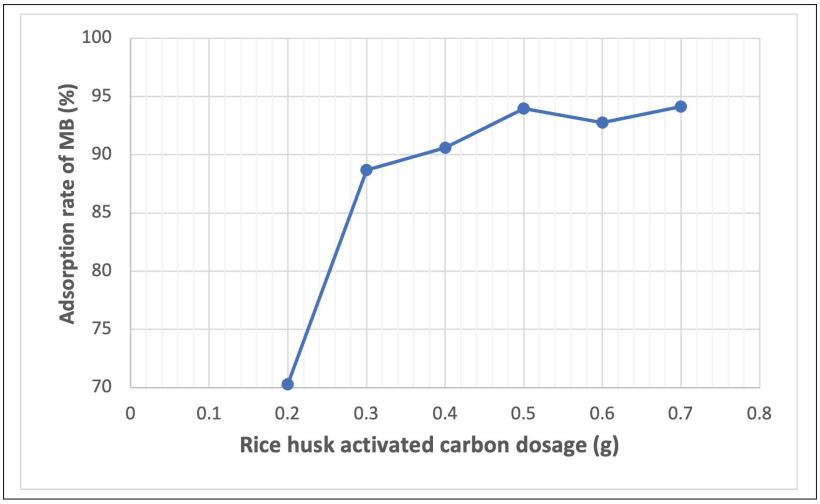

Figure 3.4 The impact of rice husk activated carbon dosages (0.2, 0.3, 0.4, 0.5, 0.6 and 0.7 g) on the methylene blue removal (pH = 11, Contact time = 12 hours, agitation speed = 150 rpm, 25°C)

by the slight dip at 0.6 g. The data comparisons underscore the direct relationship between the quantity of produced activated carbon and the percentage of methylene blue removal.

3.7 The kinetics study of the process

To investigate color removal, a set of kinetic and equilibrium trials were systematically done twice, and the mean findings were subsequently computed. The inquiry considered both the duration of contact and the initial concentration of dye. The kinetic study's foundation was formed by treating 0.3 g of rice husk-based activated carbon in the figures below with four different concentrations (30, 40, 50, and 70 $mg{\cdot}L^{-1}$) of a 500 mL methylene blue solution as the adsorbate. At optimized pH 11.0, the mixing time was constantly kept constant at 72 hours, with an agitation speed of 150 rpm. The acquired kinetic data aims to evaluate the applicability and effectiveness of various reaction models, including the pseudo-first-order reaction model, pseudo-second-order reaction model, intraparticle diffusion model, and the Elovich model. This analysis is conducted to gain deeper insights into the dynamics of the adsorption kinetics during the process.

3.7.1 Pseudo-first-order kinetic model

The figures relating to the pseudo-first-order model for the removal of methylene blue dye four different concentrations (30, 40, 50 and 70 mg·L^{-1}) with RH-based activated carbon in 25°C.

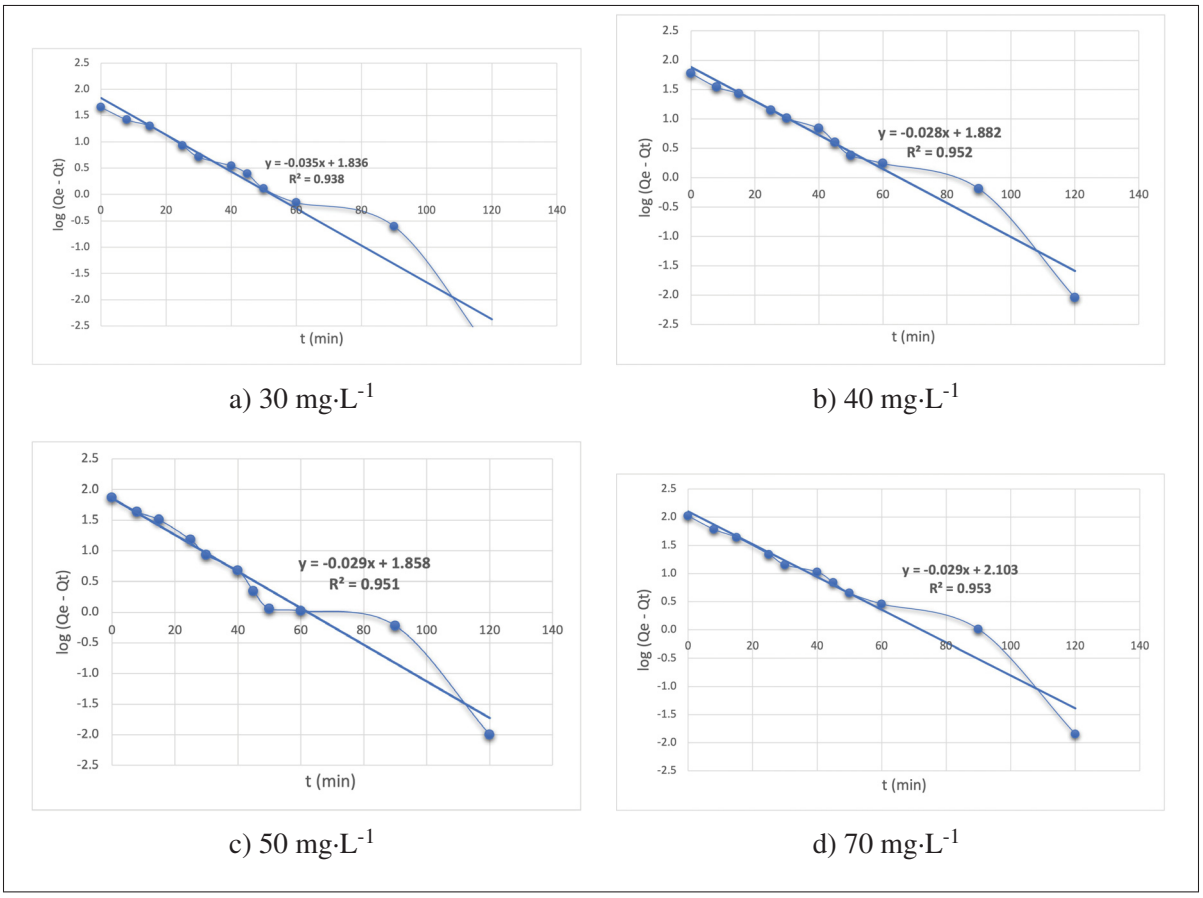

Figure 3.5 Comparison of the pseudo-first-order kinetic model at different concentrations of methylene blue at 30, 40, 50 and 70 mg·L^{-1}, pH = 11, contact time = 72 hours, agitation speed = 150 rpm and 0.3 g of rice husk activated carbon at 25°C

The equilibrium time is 73 hours while shaking at 150 rpm, pH = 11.0 appropriate RH-activated carbon is exhibited above. This particular kinetic isotherm will be explored in subsequent sections.

3.7.2 Pseudo-second-order kinetic model

The figures relating to the pseudo-second-order model for the removal of methylene blue dye four different concentrations (30, 40, 50 and 70 mg·L^{-1}) with RH-based activated carbon, 25°C, equilibrium time = 73 hours while shaking at 150 rpm.

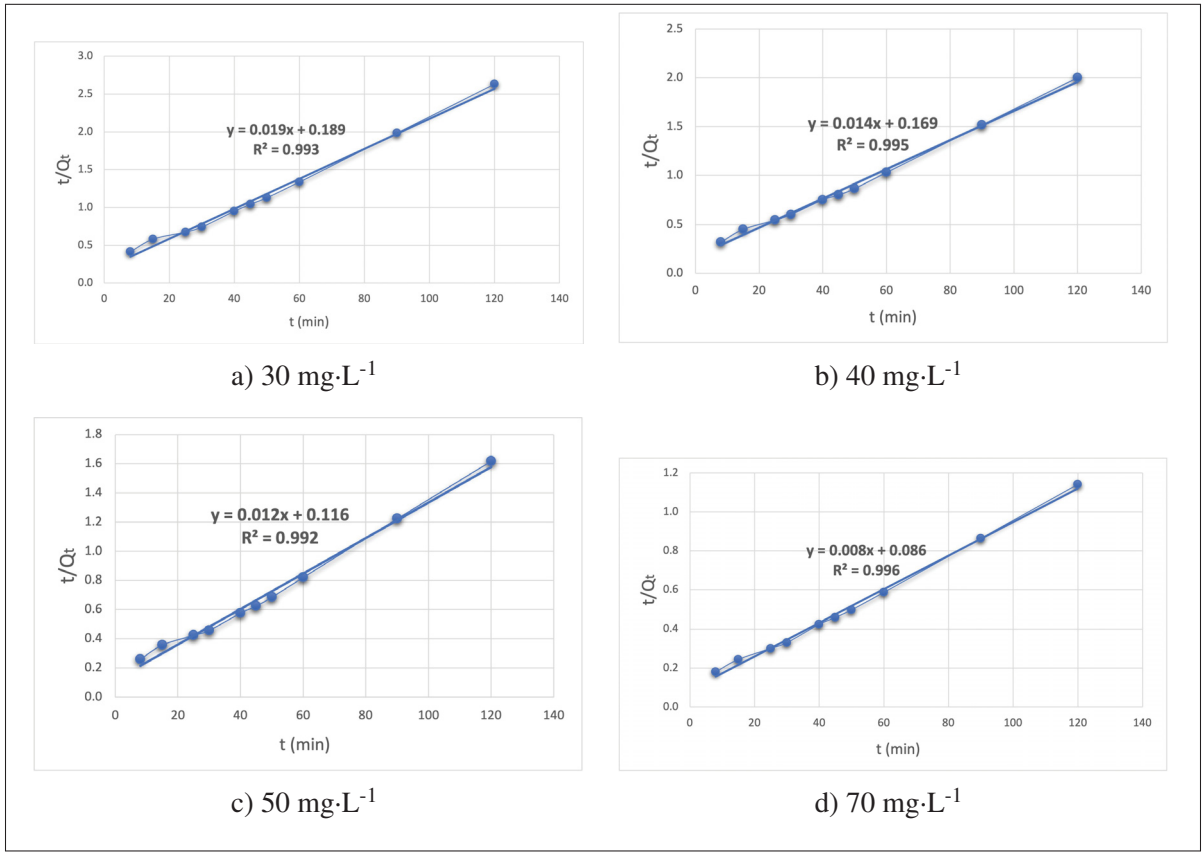

a) 30 mg·L^{-1} b) 40 mg·L^{-1}

c) 50 mg·L^{-1} d) 70 mg·L^{-1}

Figure 3.6 Comparison of the pseudo-second-order kinetic model at different concentrations of methylene blue (30, 40, 50 and 70 mg·L^{-1} at pH = 11, contact time = 72 hours, agitation speed = 150 rpm, 0.3 g of rice husk activated carbon at 25°C)

The pH = 11.0 appropriate for RH activated carbon is considered as the previous kinetic model examination.

3.7.3 Intraparticle diffusion kinetic model

The figures relating to the Intraparticle diffusion model for the removal of methylene blue dye four different concentrations (30, 40, 50 and 70 mg· L^{-1}) with RH-activated carbon, 25°C, equilibrium time = 73 hours while shaking at 150 rpm, pH = 11.0 appropriate RH-activated carbon is exhibited as follows:

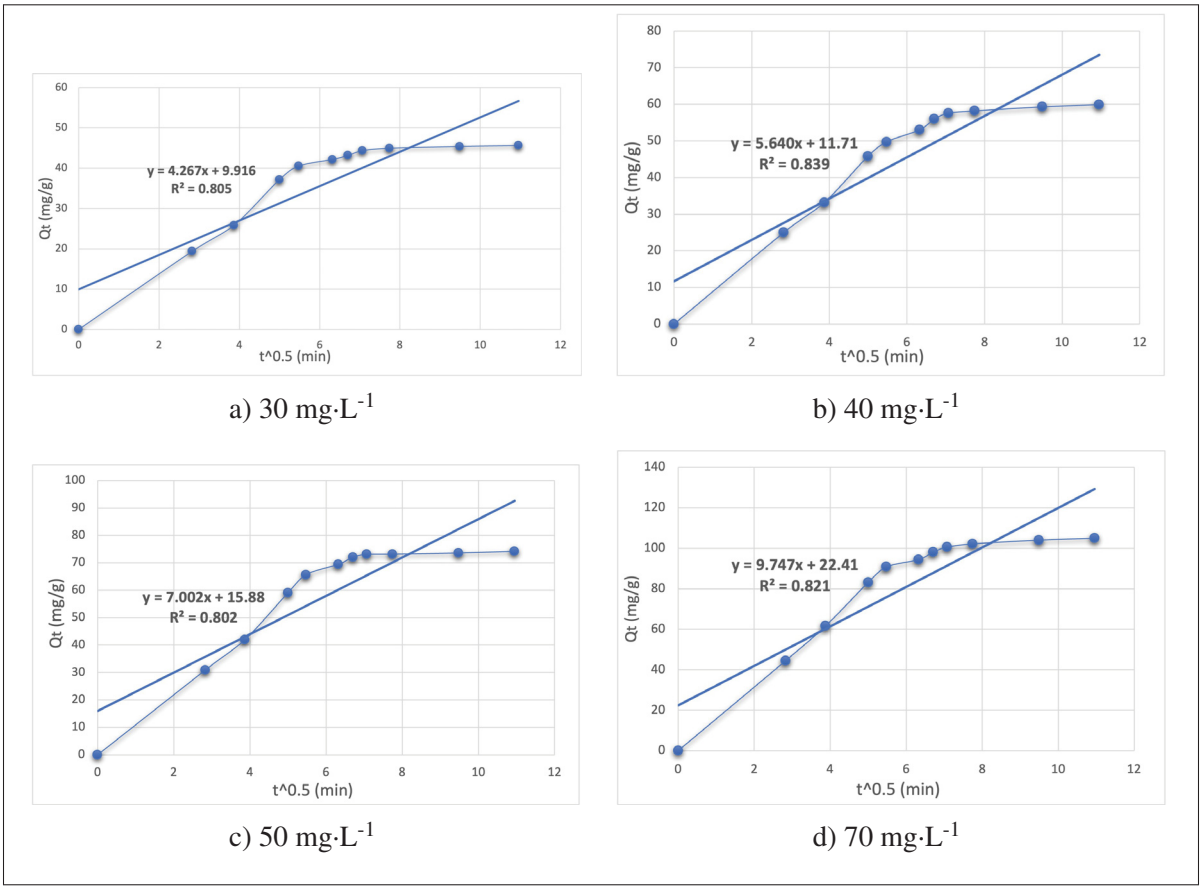

a) 30 mg·L^{-1} b) 40 mg·L^{-1}

c) 50 mg·L^{-1} d) 70 mg·L^{-1}

Figure 3.7 Comparison of the Intraparticle diffusion kinetic model at different concentrations of methylene blue (30, 40, 50 and 70 mg·L^{-1} at pH = 11, contact time = 72 hours, agitation speed = 150 rpm, 0.3 g of rice husk activated carbon at 25°C)

3.7.4 Elovich kinetic model

The figures relating to the Elovich model for the removal of methylene blue dye four different concentrations (30, 40, 50 and 70 mg·L^{-1}) with RH-based activated carbon, 25°C, equilibrium time = 73 hours while shaking at 150 rpm, pH = 11.0 appropriate RH-activated carbon is exhibited as follows:

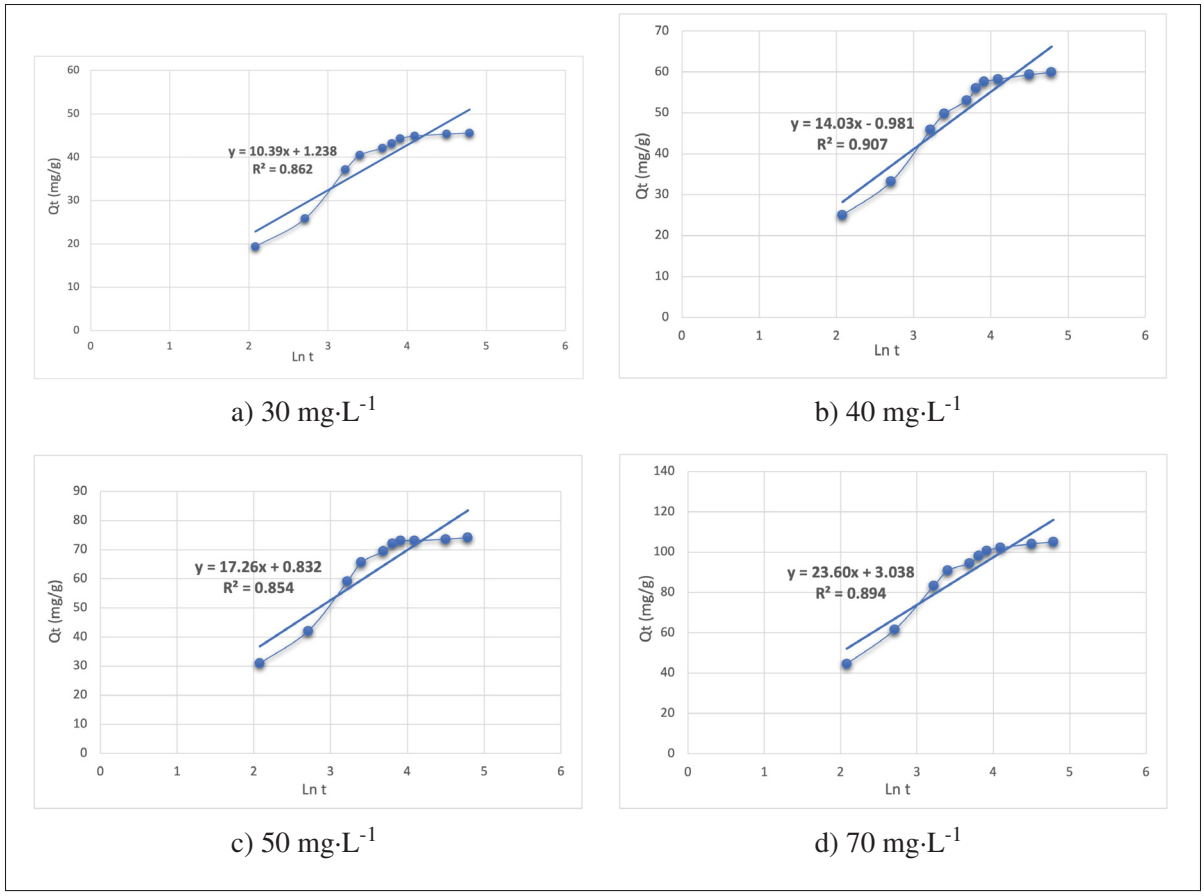

a) 30 mg·L^{-1} b) 40 mg·L^{-1}

c) 50 mg·L^{-1} d) 70 mg·L^{-1}

Figure 3.8 Comparison of the Elovich kinetic model at different concentrations of methylene blue (30, 40, 50 and 70 mg·L^{-1} at pH = 11, contact time = 72 hours, agitation speed = 150 rpm, 0.3 g of rice husk activated carbon at 25°C)

3.8 Kinetic models comparison

In the upcoming Table 3.6, diverse concentrations will be examined using different kinetic models, and the focus will be on comparing the corresponding R^2 coefficients. This comparative analysis aims to identify the most suitable kinetic model for the dye model and the prepared precursor.

Table 3.6 The kinetic model data for different concentrations of methylene blue (30, 40, 50 and 70 $mg{\cdot}L^{-1}$ and 0.3 g of rice husk activated carbon)

Pseudo 1st Order Kinetic Model							
Batch number	Concentration ($mg{\cdot}L^{-1}$)	Slope	Intercept	K_f	q_e	Q_e (exp)	R^2
1	30.0	-0.03	1.84	0.08	68.7	45.6	0.94
2	40.0	-0.03	1.88	0.08	76.3	59.9	0.95
3	50.0	-0.03	1.86	0.08	72.2	74.2	0.95
4	70.0	-0.03	2.10	0.08	126	105	0.95
Pseudo 2nd Order Kinetic Model							
Batch number	Concentration ($mg{\cdot}L^{-1}$)	Slope	Intercept	K_s	q_e	Q_e (exp)	R^2
1	30.0	0.02	0.19	0.00	50.5	45.6	0.99
2	40.0	0.01	0.16	0.00	67.1	59.9	0.99
3	50.0	0.01	0.12	0.00	81.9	74.2	0.99
4	70.0	0.00	0.09	0.00	116	105	0.99
Intraparticle Diffusion Kinetic Model							
Batch number	Concentration ($mg{\cdot}L^{-1}$)	Slope	Intercept	K_p	C	R^2	
1	30.0	4.26	9.92	4.26	9.91	0.80	-
2	40.0	5.64	11.7	5.64	11.7	0.84	-
3	50.0	7.00	15.9	7.00	15.9	0.80	-
4	60.0	9.74	22.4	9.74	22.4	0.82	-
Elovich Kinetic Model							
Batch number	Concentration ($mg{\cdot}L^{-1}$)	Slope	Intercept	α	β	R^2	
1	30.0	10.4	1.24	11.7	0.10	0.86	-
2	40.0	14.0	-0.98	13.1	0.07	0.90	-
3	50.0	17.3	0.83	18.1	0.05	0.85	-
4	70.0	23.6	3.04	26.8	0.04	0.89	-

The Lagergren model, also referred to as the pseudo first-order expression, is a well-established analytical tool employed in the investigation of adsorption kinetics (Figure 3.5). Our study leverages this model to explore the relationship between the difference in the equilibrium adsorbate concentration (q_e-q_t) and the time elapsed (t). Our empirical results consistently

demonstrate a strong correlation, as denoted by an R^2 coefficient within the range of 0.94 to 0.95, as visually represented in figure 3.5. This model facilitates the determination of essential parameters, including the rate constant (k_f) and the equilibrium adsorption capacity (q_e), which are extracted from the plot's slope and intercept, respectively. The critical rate constant (k_f) with the value of 0.08 for various concentrations of activated carbon are thoroughly documented in Table 3.6.

In our endeavor to distinguish between kinetics dependent on sorbent concentration and those influenced by solute concentration, we have employed a pseudo-second-order rate expression to evaluate the adsorption kinetics of activated carbon. Our approach involves plotting t/q_t against time (t), revealing a strong correlation with a commendable R^2 value consistently within the range of 0.99 as evidenced in the associated figures (Figure 3.6). This methodology has enabled us to determine the rate constants associated with pseudo-second-order kinetic models for different varieties of activated carbon, which are meticulously cataloged in Table 3.6. This kinetic model has shown the highest compatibility and fitted the best compared to the rest of the kinetic models.

Moreover, we have delved into the prospect of intraparticle diffusion through the application of the intraparticle diffusion model, with the findings comprehensively detailed in Table 3.6, Our examination involves plotting the logarithm of a parameter denoted as "R" against the logarithm of time (t) in Figure 3.7. Impressively, this analysis consistently illustrates an exceptionally robust correlation, as underscored by an R^2 value consistently within the remarkable range of 0.80 to 0.84, as visually elucidated in the corresponding figure 3.7. Furthermore, the rate constants specific to this unique kinetic model are thoughtfully presented within Table 3.6 enhancing our understanding of the intricacies underpinning the adsorption processes under investigation.

We used a similar method, extending our analysis to the Elovich kinetic model, and plotted the data to determine the correlation between $\ln(q_t)$ and t (Figure 3.8). As a result, Figure 3.8 shows a strong connection, which is supported by high R^2 values which are in the range of

0.85 to 0.90 and are closely like those found in the pseudo-second-order analysis. These results allow us to derive the corresponding rate constants (α and β) for the Elovich kinetic model , which contributes to our comprehension of the complex dynamics controlling the adsorption kinetics of activated carbon in different experimental scenarios. Figure 3.9 below demonstrates a comparison among the R^2 value for four different concentrations in pseudo-second-order.

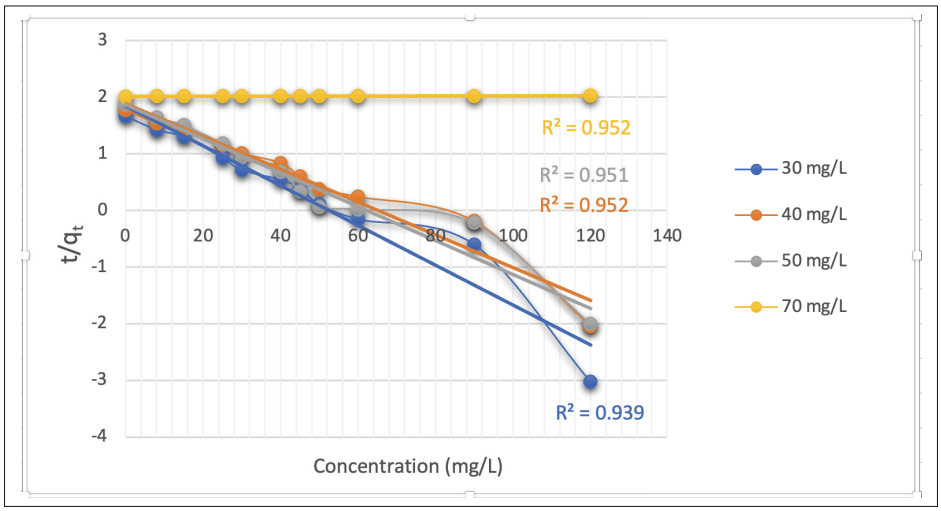

Figure 3.9 Comparison of pseudo second order kinetic model for RH-activated carbon (0.3 g) for different concentrations of methylene blue (30, 40, 50, 70 $mg{\cdot}L^{-1}$); 25°C, pH = 11.0 agitated for 73 h at 150 rpm

Figure 3.9 appears to plot the (t/q_t) ratio against concentration. Multiple data points are plotted, and four linear trend lines are referred to concentrations (30, 40, 50 and 70 $mg{\cdot}L^{-1}$), each with a corresponding coefficient of determination R^2 are shown in the figure. These values are extremely high (0.996, 0.992, 0.995, 0.993) indicating that the linear models provide an excellent fit to the data. High R^2 values close to 1 indicate that the model used to fit the data accurately describes the observed phenomenon. The trend lines are ascending which demonstrates that the ratio of time to quantity adsorbed t/q_t increases over time, suggesting a proportional relationship between time and the inverse of the adsorption capacity at time (t). This is characteristic of pseudo-second-order kinetics in adsorption processes, where the rate of occupation of adsorption sites is proportional to the square of the number of unoccupied sites.

3.9 The isotherm study of the process

In this study, we delve into an extensive examination of various isotherm models applied to the precursor in dye removal, with a primary focus on comparing their performance based on R^2 coefficients. The isotherm models under scrutiny include Langmuir, Freundlich, BET and Temkin. By meticulously analyzing and contrasting the R^2 coefficients derived from each model at different concentrations, we aim to discern which isotherm model best encapsulates the adsorption behaviour of the RH precursor. The R^2 coefficients serve as valuable indicators of the goodness of fit, enabling us to quantitatively evaluate the appropriateness of each isotherm model in representing the experimental data. This comparative analysis not only aids in unravelling the intricacies of adsorption dynamics but also guides us in identifying the most fitting isotherm model for the efficient removal of MB dye from the studied precursor.

3.10 Comparison between four different studied isotherm models

In this process, a fixed quantity of 3 g of the adsorbent was mixed with varying concentrations of the methylene blue solution (30, 40, 50, and 70 $mg{\cdot}L^{-1}$) in separate 500 mL volumes. Each mixture was agitated at 150 rpm at pH = 11 for a continuous duration of 72 hours until equilibrium was achieved across all samples.

Based on the figures presented below (Figure 3.10), we have conducted a comparative analysis of the adsorption of RH-activated carbon at varying concentrations. In these experiments, a consistent amount of activated carbon (0.3 g) was employed, with methylene blue serving as the chosen dye for assessing adsorption capacity. Utilizing linear regression analysis, we calculated isotherm parameters and the coefficient of determination (R^2). The results for different isotherm models are detailed in the accompanying table (Table 3.7). The maximum adsorption capacity (q_{max}) of methylene blue on RH-activated carbon was determined to be 285 $mg{\cdot}g^{-1}$ at 30°C according to the Langmuir isotherm model.

As the initial solution concentrations of methylene blue increase, the remaining concentration of methylene blue in the solution after adsorption also increases. However, the amount of methylene

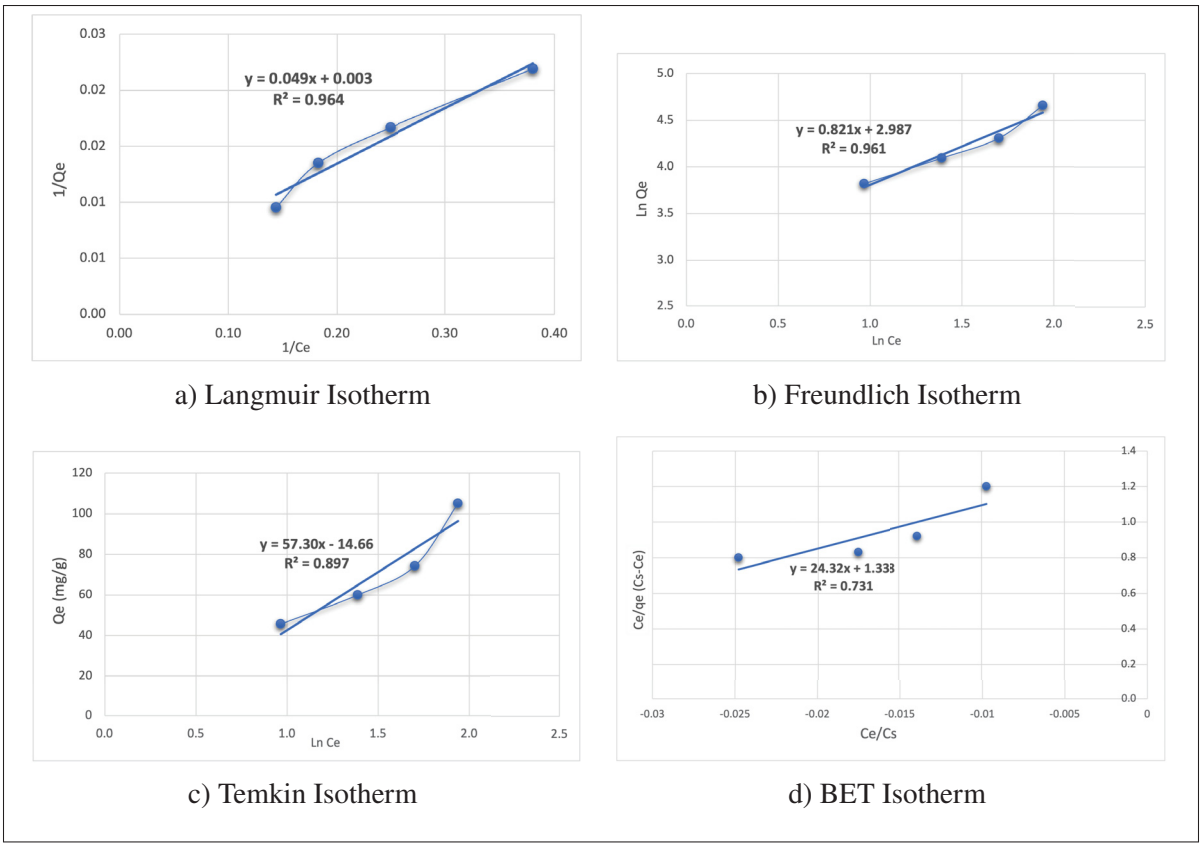

Figure 3.10 Langmuir, Freundlich, Temkin and BET isotherm models for the removal of methylene blue dye with rice husk activated carbon, 25°C, equilibrium time = 73 h while shaking at 150 rpm, pH = 11.0 appropriate for rice husk activated carbon

blue adsorbed (q_e) remains relatively constant. This observation suggests that the adsorption process of methylene blue onto RH-activated carbon is limited to monolayer adsorption, aligning with the predictions of the Langmuir model. Additionally, the equilibrium isotherm constants and correlation coefficients, derived from linear fits of both Langmuir and Freundlich isotherms, are provided in Table 3.7 Linear regression was employed to estimate these parameters, and the R^2 values ranged from 0.80 to 0.98, indicating a good fit of adsorption to all isotherm models. These data illustrate that a higher adsorbate concentration (70 mg·L^{-1}) corresponds to improved fits for both the isotherm and kinetic models.

It is worth noting that the produced activated carbon exhibited a stronger correlation with the Langmuir and Freundlich isotherms compared to the BET and Temkin isotherms. R square (R^2)

Table 3.7 Isotherm models experimental data of rice husk-based onto adsorbate MB

Isotherm Models	Q_e experimental ($mg \cdot g^{-1}$)	Parameters	Linear form
Langmuir	285	K_L ($mg \cdot L^{-1}$)	0.07
		R_L	0.32 (30 $mg \cdot L^{-1}$)
		R^2	0.96
		Slope	0.04
		Intercept	0.00
Freundlich	285	n	1.21
		K_L ($mg \cdot g^{-1}$)($L \cdot mg^{-1}$)$^{1/n}$	19.8
		R^2	0.96
		Slope	0.82
		Intercept	2.98
Temkin	285	K_T	0.77
		B	57.3
		Slope	57.3
		Intercept	-14.6
		R^2	0.89
BET	285	Slope	24.3
		Intercept	1.34
		R^2	0.78

represents the coefficient of determination, a statistical metric assessing the degree to which the experimental data aligns with the isotherm and kinetic models. This observation is based on correlation coefficients exceeding 0.95 across four distinct batches with differing concentrations (30, 40, 50 and 70 $mg \cdot L^{-1}$)(Gundogdu et al., 2012).

In the context of the Langmuir isotherm (Table 3.7), R_L serves as the separation factor. R_L is less than 1, signifying favourable adsorption. The favourable nature of methylene blue adsorption onto RH-activated carbon may be shown by the fact that all R_L values are lower than 1. Based on these findings, the RH-activated carbon exterior and pore surfaces had uniformly distributed binding sites during the activation phase (Unur, 2013). This suggests that as the initial concentration (C_i) increases, the adsorption capacity also increases. In such a scenario, the adsorption process is efficient when described by this isotherm model.

In the context of the Freundlich isotherm, the parameter 'n' offers valuable insights into the characteristics of the adsorption process. When 'n' exceeds 1 ($n > 1$), it signifies favourable

and increasingly robust adsorption. This indicates that adsorption becomes more pronounced at higher adsorbate concentrations, suggesting a heterogeneous surface for the adsorbent. The BET isotherm model indicates that the transition from monolayer to multilayer adsorption is unlikely, and it is the most appropriate model when monolayer adsorption takes place. Consequently, it is the least suitable fit for the adsorption model, following the Temkin isotherm model.

3.11 The morphological observation (SEM image)

Scanning electron microscopy (SEM) analysis was used to conduct the morphological analyses of activated carbon. After carefully reviewing the images, it becomes apparent that the activated carbon derived from rice husk displays a diverse particle size distribution, accentuating its inherently granular composition. The presence of irregularities and variations in particle size is a noteworthy feature, significantly contributing to the material's overall efficacy in adsorbing a wide array of contaminants. Notably, in the image (b), distinctive jagged edges and open pores are observable, elevating the material's adsorption capacity. These characteristic pores, stemming from the intricate activation process, play a pivotal role in enhancing the material's performance.

Furthermore, in figure 3.11, the image (b) displays a well-developed network of macropores, mesopores, and micropores that together provide a large surface area that increases the adsorption capacity of the material. The homogeneous dispersion of pores throughout the surface indicates a regulated activation procedure, guaranteeing reliable and effective adsorption sites all over the substance. Examining the images (c and d), you can see that the material's high surface area is mostly attributed to the cavities that have been found. The network of interconnected pores forms a labyrinthine structure that maximizes the number of adsorption sites available and, as a result, increases the activated carbon's overall efficiency. This feature is also advantageous for rapid adsorption kinetics and effective utilization of the entire porous network. In image (a), the porous structure is clearly evident.

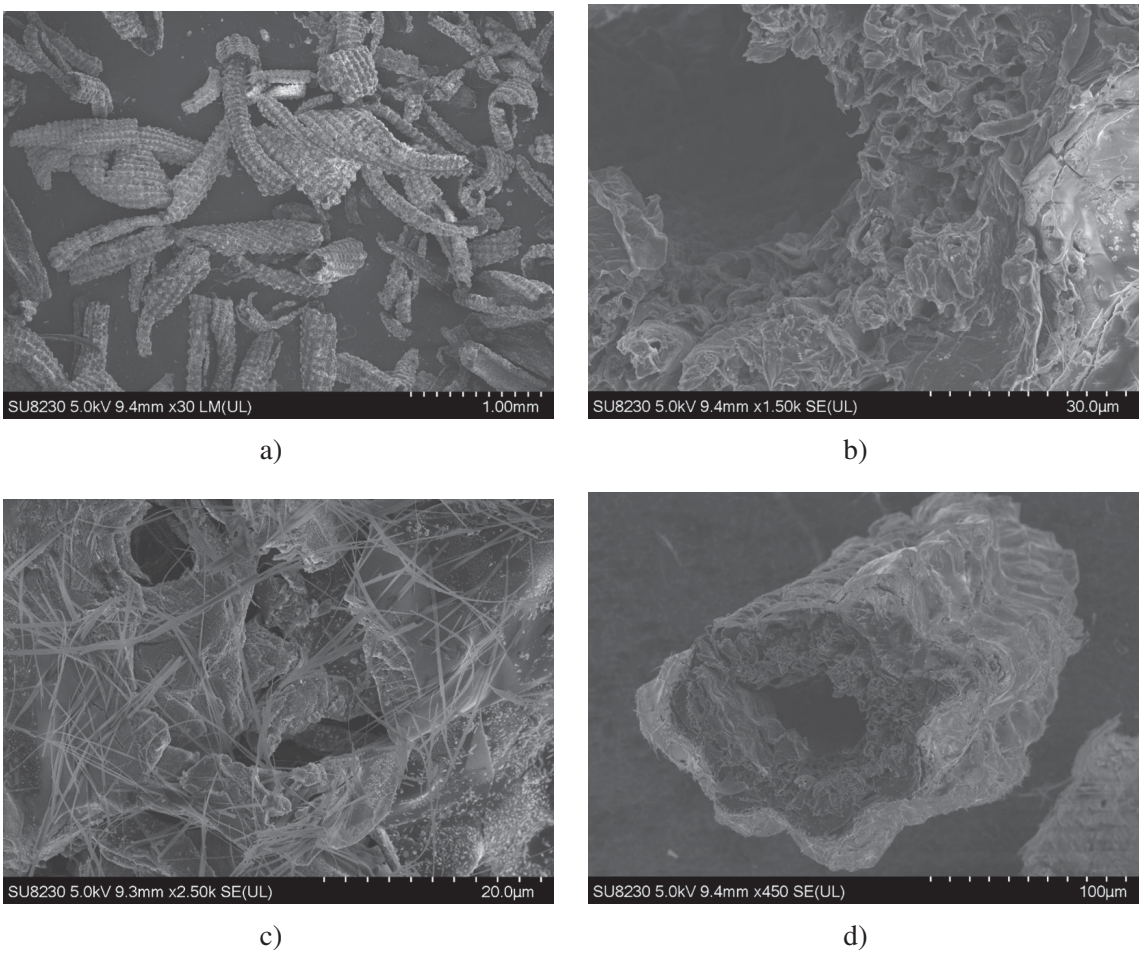

Figure 3.11 SEM images a (1.00 mm), b (30.0 µm), c (20.0 µm) and d (100 µm)

CHAPTER 4

DISCUSSION

In this discussion, we will examine the experimental results in great detail and interpret the nuances of producing activated carbon from rice husk. The adsorption capacity of the produced activated carbon will be determined by analyzing the results of the iodine and methylene blue adsorption tests. By carefully investigating these findings, we want to shed light on the effects of important parameters on the characteristics of the final product, including temperature, contact time, and the combined carbonization and activation process. Understanding how the selected parameters affect the efficacy and efficiency of activated carbon synthesis is made possible by this study.

4.1 Rice husk as a source for activated carbon

The synthesis method involves the gasification of rice husk using sugarcane bagasse, another cost-effective agricultural byproduct, as a source of carbon dioxide (CO_2) in an oxygen-based environment to activate the carbon. This process employs a technique known as the two crucible method which minimizes the use of oxygen while utilizing CO_2 as an oxidizing agent. This approach enhances the development of activated carbon with improved porosity and a substantial surface area, making it suitable for various treatment applications.

Rice husk-derived activated carbon has undergone testing for the removal of methylene blue dye and determining the iodine number. The results from batch experiments demonstrated that this activated carbon exhibited an maximized adsorption rate for the specific dye solution under the study. In the activation process, sugarcane bagasse, an agricultural residue, serves as an activating agent, contributing to the creation of an efficient adsorbent within an oxygen-based environment.

With sugarcane bagasse serving as the activating agent, it is possible to produce activated carbon from inexpensive rice husk in an atmosphere without the need for inert gases such as nitrogen or

argon gas. The exploitation of rice husk, a frequently available agricultural byproduct, proposes a sustainable strategy. However, the efficacy of the activated carbon depends on several aspects, such as activation conditions.

4.2 Comparison with existing literature

The studies referenced offer a diverse array of methodologies and outcomes in the realm of rice husk-based activated carbon production. Alvarez et al., 2015 underscore the importance of CO_2 activation for enhancing the microporous structure of activated carbon derived from rice husk, citing its superiority over steam activation. This approach is lauded for its cleanliness, ease of handling, and precise control, particularly at temperatures around 800°C due to the relatively slow reaction rate of CO_2 (Ioannidou and Zabaniotou, 2007). Conversely, the study employing $ZnCl_2$ activation, Kalderis et al., 2008 opts for a swift, single-stage chemical activation process, yielding activated carbons with notable surface areas of 674 $m^2 \cdot g^{-1}$ for bagasse and 750 $m^2 \cdot g^{-1}$ for rice husk. This study highlights the efficacy of $ZnCl_2$ as an impregnating agent and the importance of optimizing activation temperature for surface area enhancement.

Meanwhile, another investigation utilizing response surface methodology (RSM) (Zhang et al., 2017) takes a systematic approach to optimizing activated carbon production variables. Through rigorous experimentation and analysis, this study identifies activation temperature as the most influential parameter affecting iodine adsorption capacity. By achieving an impressive iodine adsorption capacity of 970 $mg \cdot g^{-1}$ under optimized conditions, this study demonstrates the potential for fine-tuning activation parameters to maximize adsorption performance.

In contrast, this study places a specific emphasis on iodine adsorption capacity optimization through an integrated carbonization and activation process. Under carefully controlled conditions (activation temperature: 710°C, activation time: 30 min, heating rate: 10°C·min^{-1}), remarkable results are achieved, including an iodine adsorption capacity of 836 $mg \cdot g^{-1}$, a methylene blue adsorption capacity of 285 $mg \cdot g^{-1}$, and a char yield of 31.5%. By prioritizing iodine adsorption capacity while considering sustainability aspects, this study offers a unique perspective on

activated carbon production from rice husk. Furthermore, the findings from studies such as those focusing on simultaneous silica and activated carbon production. Liou and Wu, 2009 contribute to the broader understanding of rice husk utilization, highlighting its potential for multifunctional applications and sustainable resource management.

Together, these findings contribute to understanding rice husk utilization. Importantly, Langmuir and Freundlich isotherms and pseudo-second-order as the main kinetic model proved to be fitting models, providing a robust framework for comprehending adsorption behavior across these studies, including our own pursuit of sustainable activated carbon production from rice husk (Menya et al., 2018).

4.3 The utilization of the generated activated carbon

The production of rice husks as activated carbons is considered important in many nations, especially those where rice cultivation is significant. This reasonably priced activated carbon could be advantageous for nations like Vietnam, Thailand, China, India, and others that have substantial agricultural industries. Activated carbon has the potential to be utilized in the remediation of organic pollutants, dyes, and other compounds found in water and air. When evaluating rice husk's potential to be converted into activated carbon, it is important to consider local environmental laws, infrastructure, and raw material availability.

This study establishes that the physically and chemically activated plant exhibits a great adsorptive capacity for dyes. The iodine number values indicate that the incorporation of sugarcane bagasse as an activating agent in the carbonization/activation process not only results in a substantial increase in surface area but also underscores the significant contribution of microporosity to the overall surface area of the prepared activated carbon. This renders it an effective adsorbent for dye removal. Importantly, the efficient removal of methylene blue by these adsorbents underscores its suitability for treating colored effluent waters.

4.4 Significance and delineation of the Study

This research is significant since it aims to address environmental issues and improve wastewater treatment technologies. The elaborate procedures involved in conventional systems often create issues for sustainability. This work intends to contribute to a paradigm shift, supporting ecologically friendly wastewater treatment solutions, by investigating novel methodologies and employing sustainable materials such as rice husk and sugarcane bagasse.

The delineation of this research focuses on evaluating the production of activated carbon using agricultural waste materials, specifically rice husk. The production process involves three key stages:

Preparation of Sustainable Precursors: The initial stage involves washing and sieving rice husk to create sustainable precursors.

Acid-Base Leaching Method: The second stage employs an acid-base leaching method under atmospheric conditions to enhance the quality of the resulting activated carbon.

Integrated Carbonization and Activation: The third stage involves an integrated process of carbonization and activation carried out under normal atmospheric conditions, culminating in the production of the final activated carbon product.

The research also includes the following steps:

Surface Area and Pore Volume Evaluation: The surface area and pore volume of the manufactured activated carbon are assessed using iodine adsorption and methylene blue adsorption tests.

Optimization: The obtained results are optimized, and all relevant variables are outlined. Through these stages, the research investigates the entire production process, assessing its potential for generating activated carbon from agricultural waste materials.

4.5 Processes involved in this research

The experimental procedures investigated in this study encompass the following aspects:

Surface Enhancement of Precursors: Prior to the activation phase, the enhancement of precursor surfaces is explored.

Adsorption Capacity Analysis: The adsorption capacity of the produced adsorbent is assessed using an iodine adsorption test.

Influence of Production Factors: Various influential factors such as activation time, activation temperature, acid/base leaching duration, heating rate and the initial weight of the physical agent (sugarcane bagasse) and the rice husk as the precursor in the production process are examined to achieve optimization of adsorbent characteristics and quality.

Adsorption Process Investigation: The adsorption process is described and studied. Multiple isotherm parameters are compared to identify the most suitable isotherm and kinetic model based on their coefficients (R^2).

These experimental processes collectively contribute to a comprehensive exploration of various stages in the production and characterization of the adsorbent material, encompassing surface enhancement, adsorption capacity analysis, production factor optimization, and the detailed investigation of the adsorption process itself.

4.6 Limitations and recommendations

There are a few constraints to the study to take into account. The research is mainly focused on specific supplies of rice husk and sugarcane bagasse as an activating agent, which may limit the generalizability of the findings to other regions and alternative raw materials. Furthermore, there are still unknowns regarding the proposed method's scalability for large-scale production, as well as possible difficulties in moving from laboratory-scale research to industrial-scale applications. There is a degree of uncertainty when comparing results with other research or

practical applications because of the diversity in adsorption testing conditions such as starting concentrations and temperature. Moreover, a thorough temporal investigation of the durability and long-term effectiveness of the produced activated carbon has been excluded from the study.

Recommendations for future research include exploring the method's applicability to diverse agricultural residues, conducting pilot-scale studies, standardizing testing conditions, and integrating long-term stability assessments and economic analyses. Additionally, sensitivity analyses on key activation parameters and optimization for reproducibility should be priorities in refining the proposed methodology.

CONCLUSION AND RECOMMENDATIONS

In conclusion, the goal of this extensive study was to maximize the effectiveness of activated carbon derived from rice husks in the removal of methylene blue (MB). The study methodically investigated several variables such as activation temperature and time, acid and base leaching period and the initial weights of the precursor and the activating agent, illuminating crucial elements affecting the adsorption process and offering insightful information for real-world uses in environmental remediation and wastewater treatment.

By using rice husk and sugarcane bagasse, this research has effectively used a novel and less technically restrained method to produce activated carbon. Ttwo crucible method is used in the gasification process to produce activated carbon with increased porosity and a large surface area. The carbon is produced using bagasse from sugarcane. Adding sugarcane bagasse as an activating agent helps create an effective adsorbent in an atmospheric environment while also streamlining the manufacturing process.

The iodine number of each resulting activated carbon has been determined, and the optimal conditions for the generation of RH-activated carbon have been identified. Specifically, the optimal activation temperature is set at 700°C, with an acid/base leaching duration of 2 hours involving continuous stirring at 150 rpm. The initial weights of both rice husk and sugarcane bagasse are established at 10 g, and the heating rate is maintained at $10°C \cdot min^{-1}$. Under these carefully selected parameters, the achieved iodine number reaches its peak at 836 $mg \cdot g^{-1}$, accompanied by a char yield of 31.5% and methylene blue removal rate at 94.1 %. This outcome represents the highest observed adsorption capacity for the precursor, highlighting the effectiveness of the chosen conditions in enhancing the adsorption properties of the activated carbon derived from rice husk and sugarcane bagasse.

Higher temperatures cause more volatile matter to be released, which lowers the char yield. The char yield was clearly influenced by the heating rates. The formation of activated carbon is more

complete when the reaction time is longer, and the heating rate is lower. The biochar developed a carbonous structure at temperatures between 500 and 700 °C, and this had a negative correlation with the rate of char yield.

The analysis of adsorbent dosages indicated that the percentage of dye removal and the amount of activated carbon have a significant connection. The results provided critical information for the useful application of activated carbon in treatment processes by highlighting the significance of establishing an ideal dosage that strikes a compromise between increased adsorption capacity and financial considerations.

The effect that pH had on the removal process highlighted how important it is to adjust ambient factors based on the type of adsorbent. Adjusting pH is crucial to achieve the best removal results, as seen by the tendency of increased dye removal efficiency with increasing pH levels, especially in alkaline conditions.

The analysis of contact time demonstrated how important it is to determine ideal adsorption capacity. Indicating the saturation of active binding sites on the activated carbon and highlighting the significance of equilibrium in reaching maximal adsorption capacity, the data showed a steady improvement in removal effectiveness with extended contact times.

The investigation shows that better fits for both isotherm and kinetic models are obtained at a greater adsorbate concentration of 70 $mg \cdot g^{-1}$. This finding, which suggests that the adsorption process can be adjusted by varying the starting concentration, is critical for real-world applications. Furthermore, the Langmuir and Freundlich models show better correlations with the experimental data than the BET and Temkin models, which further supports their suitability for explaining the adsorption process, according to the comparison of isotherm models.

When compared to Langmuir and Freundlich isotherms, the generated RH-activated carbon shows remarkably consistent correlations across various batches and concentrations. Strong

agreement between the experimental data and the isotherm and kinetic models is indicated by the robust correlation coefficients greater than 0.95. These findings advance our knowledge of the adsorption process and offer useful information for developing effective adsorption systems that use rice husk-activated carbon to remove methylene blue from the sample.

Pseudo-second order and Elovich models were among the many models used in kinetic studies, which shed light on the adsorption process's temporal dynamics. The excellent R^2 values that these models produced demonstrated how well they captured the complex dynamics and advanced our knowledge of the fundamental principles controlling the adsorption process.

All the results add to a comprehensive understanding of the intricate dynamics of rice husk-activated carbon adsorption for the removal of methylene blue. This information is essential for creating environmentally friendly and durable wastewater treatment and environmental protection systems. Given the circumstances, the study lays the groundwork for future investigations into customizing adsorption procedures for various contaminants and maximizing the usefulness of rice husk-activated carbon in environmental remediation.

APPENDIX I

EXPERIMENTAL DATA

1. First section of the appendix

1.1 Figures in annexes

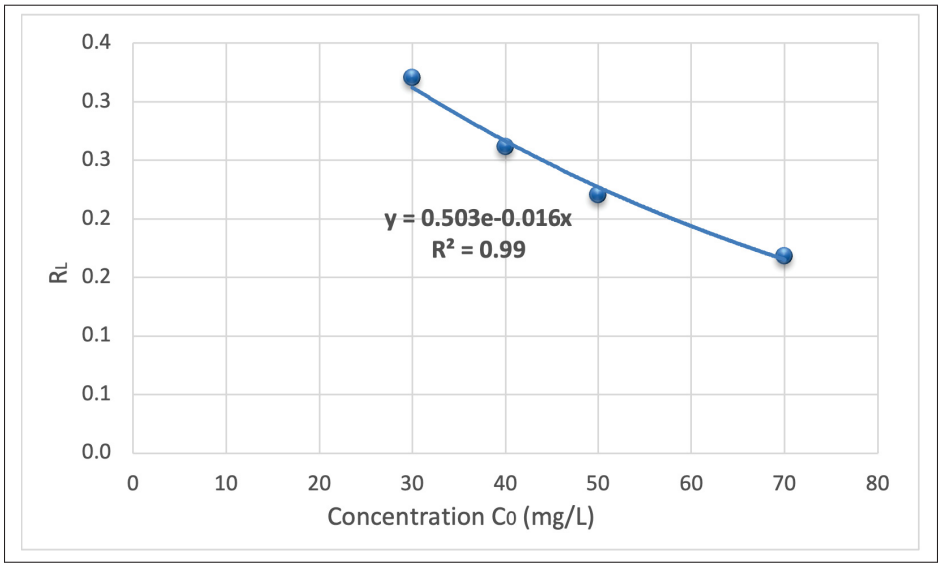

Figure-A I-1 The comparison of different concentrations of methylene blue(30, 40, 50 and 70 $mg \cdot L^{-1}$) (pH = 11 and the rice husk activated carbon dosage of 0.3 g, contact time = 73 hours, agitation speed at 150 rpm, 25°C) vs R_L

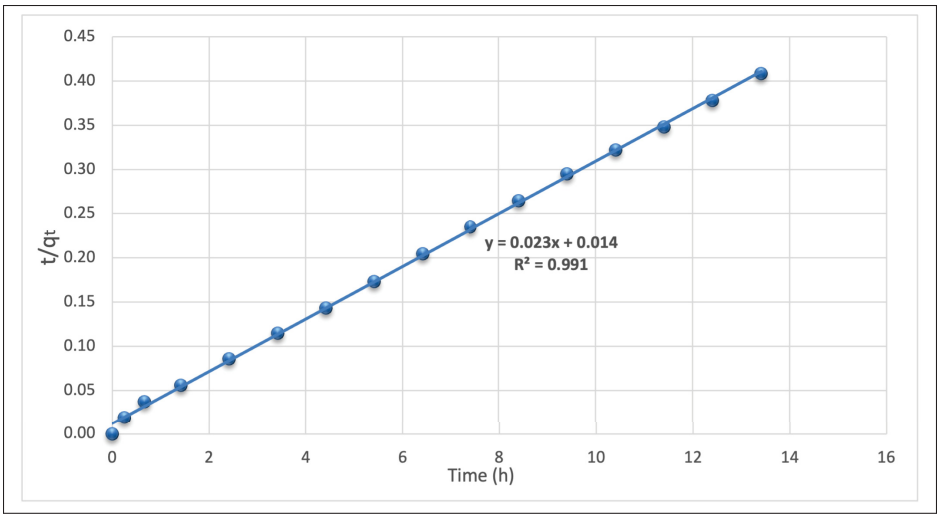

Figure-A I-2 Pseudo-second-order kinetic model for removal of methylene blue dye with RH-based activated carbon (0.3 g), 25°C, equilibrium time = 73 h while shaking at 150 rpm, pH = 11 appropriate rice husk activated carbon

1.2 Tables in annexes

Table-A I-1 Experimental Data for Adsorption Process (30 mg·L^{-1})

Time (min)	**C_0 (mg·L^{-1})**	**UV Abs**	**C_t (mg·L^{-1})**	**q_t (mg·L^{-1})**	**log(Q_e-Q_t**	**t/Q_t**	**$t^{0.5}$**	**(ln(t))**
0	30	0	0	0	1.65	-	-	0.00
8	30	0.33	18.3	19.3	1.41	0.41	2.82	2.07
15	30	0.26	14.4	25.8	1.29	0.58	3.87	2.70
25	30	0.14	7.70	37.1	0.92	0.67	5.00	3.21
30	30	0.11	5.69	40.5	0.70	0.74	5.47	3.40
40	30	0.09	4.71	42.1	0.54	0.94	6.32	3.68
45	30	0.08	4.09	43.1	0.38	1.04	6.70	3.80
50	30	0.07	3.40	44.3	0.10	1.12	7.07	3.91
60	30	0.06	3.04	44.9	-0.15	1.33	7.74	4.09
90	30	0.06	2.77	45.3	-0.60	1.98	9.48	4.49
120	30	0.05	2.62	45.6	-3.02	2.63	10.9	4.78

Table-A I-2 Experimental Data for Adsorption Process (40 mg·L^{-1})

Time (min)	**C_0 (mg·L^{-1})**	**UV Abs**	**C_t (mg·L^{-1})**	**q_t (mg·L^{-1})**	**log(Q_e-Q_t**	**t/Q_t**	**$t^{0.5}$**	**(ln(t))**
0	40	0.00	0	0	1.77	0	-	-
8	40	0.44	24.9	25.0	1.54	0.31	2.82	2.07
15	40	0.36	20.0	33.2	1.42	0.45	3.87	2.70
25	40	0.23	12.4	45.8	1.14	0.54	5.00	3.21
30	40	0.18	10.1	49.7	1.00	0.60	5.47	3.40
40	40	0.15	8.15	53.0	0.83	0.75	6.32	3.68
45	40	0.12	6.38	56.0	0.59	0.80	6.70	3.80
50	40	0.10	5.43	57.6	0.37	0.86	7.07	3.91
60	40	0.10	5.05	58.2	0.24	1.03	7.74	4.09
90	40	0.08	4.39	59.3	-0.18	1.51	9.48	4.49
120	40	0.08	4.01	59.9	-2.04	2.00	10.9	4.78

Table-A I-3 Experimental Data for Adsorption Process (50 mg·L^{-1})

Time (min)	**C_0 (mg·L^{-1})**	**UV Abs**	**C_t (mg·L^{-1})**	**q_t (mg·L^{-1})**	**log(Q_e-Q_t**	**t/Q_t**	**$t^{0.5}$**	**(ln(t))**
0	50	0.00	0	0	1.870	0	-	-
8	50	0.56	31.4	30.9	1.63	0.25	2.82	2.07
15	50	0.44	24.7	42.0	1.50	0.35	3.87	2.70
25	50	0.26	14.5	59.0	1.17	0.42	5.00	3.21
30	50	0.19	10.6	65.6	0.93	0.45	5.47	3.40
40	50	0.15	8.32	69.4	0.67	0.57	6.32	3.68
45	50	0.13	6.78	72.0	0.33	0.62	6.70	3.80
50	50	0.11	6.15	73.0	0.05	0.68	7.07	3.91
60	50	0.11	6.10	73.1	0.02	0.82	7.74	4.09
90	50	0.11	5.83	73.6	-0.22	1.22	9.48	4.49
120	50	0.10	5.48	74.2	-2.00	1.61	10.9	4.78

Table-A I-4 Experimental Data for Adsorption Process (50 mg·L^{-1})

Time (min)	**C_0 (mg·L^{-1})**	**UV Abs**	**C_t (mg·L^{-1})**	**q_t (mg·L^{-1})**	**log(Q_e-Q_t**	**t/Q_t**	**$t^{0.5}$**	**(ln(t))**
0	70	0.00	0	0	2.02	0	-	-
8	70	0.76	43.2	44.5	1.78	0.17	2.82	2.07
15	70	0.59	33.0	61.5	1.63	0.24	3.87	2.70
25	70	0.36	20.0	83.2	1.34	0.30	5.00	3.21
30	70	0.28	15.5	90.8	1.15	0.33	5.47	3.40
40	70	0.24	13.3	94.4	1.02	0.42	6.32	3.68
45	70	0.20	11.1	98.1	0.84	0.45	6.70	3.80
50	70	0.18	9.64	100	0.65	0.49	7.07	3.91
60	70	0.16	8.66	102	0.45	0.58	7.74	4.09
90	70	0.14	7.55	104	0.01	0.86	9.48	4.49
120	70	0.13	6.94	105	-1.84	1.14	10.9	4.78

BIBLIOGRAPHY

Abatan, O. G., Oni, B. A., Agboola, O., Efevbokhan, V., and Abiodun, O. O. (2019). Production of activated carbon from african star apple seed husks, oil seed and whole seed for wastewater treatment. *Journal of Cleaner Production*, 232:441–450.

Abdulmagid Basheer Agila, T., Khalifa, W. M., Saint Akadiri, S., Adebayo, T. S., and Altuntaş, M. (2022). Determinants of load capacity factor in south korea: does structural change matter? *Environmental Science and Pollution Research*, 29(46):69932–69948.

Adamson, G. (1997). *Physical Chemistry of Surfaces*. John Wiley and Sons, 6th edition.

Ahiduzzaman, M. and Sadrul Islam, A. (2016). Preparation of porous bio-char and activated carbon from rice husk by leaching ash and chemical activation. *SpringerPlus*, 5(1):1–14.

Ahmedna, MOHAMED, M. W. and Rao (2000). Production of granular activated carbons from select agricultural by-products and evaluation of their physical, chemical and adsorption properties. *Bioresource technology*, 71(2):113–123.

Ajala, E., Ighalo, J., Ajala, M., Adeniyi, A., and Ayanshola, A. (2021). Sugarcane bagasse: a biomass sufficiently applied for improving global energy, environment and economic sustainability. *Bioresources and Bioprocessing*, 8(1):1–25.

Alaya, M., Girgis, B., and Mourad, W. (2000). Activated carbon from some agricultural wastes under action of one-step steam pyrolysis. *Journal of Porous Materials*, 7:509–517.

Allen, M. . K. (1989). Intraparticle diffusion of a basic dye during adsorption onto sphagnum peat. *Environmental Pollution*, 56(1):39–50.

Alvarez, J., Lopez, G., Amutio, M., Bilbao, J., and Olazar, M. (2015). Physical activation of rice husk pyrolysis char for the production of high surface area activated carbons. *Industrial & Engineering Chemistry Research*, 54(29):7241–7250.

Amuda, O., Giwa, A., and Bello, I. (2007). Removal of heavy metal from industrial wastewater using modified activated coconut shell carbon. *Biochemical Engineering Journal*, 36(2):174–181.

Annable (1952). Application of the temkin kinetic equation to ammonia synthesis in large-scale reactors. *Chemical Engineering Science*, 1(4):145–154.

Aravindhan, R. . N. (2007). Kinetic and equilibrium studies on biosorption of basic blue dye by green macro algae caulerpa scalpelliformis. *Journal of Environmental Science and Health, Part A*, 42(5):621–631.

Ateş, F. and Özcan, Ö. (2018). Preparation and characterization of activated carbon from poplar sawdust by chemical activation: comparison of different activating agents and carbonization temperature. *European Journal of Engineering and Technology Research*, 3(11):6–11.

Aygün, A., Yenisoy-Karakaş, S., and Duman, I. (2003). Production of granular activated carbon from fruit stones and nutshells and evaluation of their physical, chemical and adsorption properties. *Microporous and mesoporous materials*, 66(2-3):189–195.

Babel, S. and Kurniawan, T. A. (2004). Cr (vi) removal from synthetic wastewater using coconut shell charcoal and commercial activated carbon modified with oxidizing agents and/or chitosan. *Chemosphere*, 54(7):951–967.

Bakar, R. A., Yahya, R., and Gan, S. N. (2016). Production of high purity amorphous silica from rice husk. *Procedia chemistry*, 19:189–195.

Barroso-Bogeat, A., Alexandre-Franco, M., Fernandez-Gonzalez, C., and Gomez-Serrano, V. (2019). Activated carbon surface chemistry: Changes upon impregnation with al (iii), fe (iii) and zn (ii)-metal oxide catalyst precursors from no3- aqueous solutions. *Arabian Journal of Chemistry*, 12(8):3963–3976.

Benjelloun, Miyah, E. Z. . L. (2021). Recent advances in adsorption kinetic models: Their application to dye types. *Arabian Journal of Chemistry*, 14(4):103031.

Bhatnagar, A. and Minocha, A. (2006). Conventional and non-conventional adsorbents for removal of pollutants from water–a review.

Bhatnagar, A., Sillanpää, M., and Witek-Krowiak, A. (2015). Agricultural waste peels as versatile biomass for water purification–a review. *Chemical engineering journal*, 270:244–271.

Brunauer, E. . T. (1938). Adsorption of gases in multimolecular layers. *Journal of the American Chemical Society*, 60(2):309–319.

Cechinel, M. A. P. and de Souza, A. A. U. (2014). Study of lead (ii) adsorption onto activated carbon originating from cow bone. *Journal of Cleaner Production*, 65:342–349.

Chen, Y., Zhu, Y., Wang, Z., Li, Y., Wang, L., Ding, L., Gao, X., Ma, Y., and Guo, Y. (2011). Application studies of activated carbon derived from rice husks produced by chemical-thermal process—a review. *Advances in colloid and interface science*, 163(1):39–52.

Chilton, Marshall, W. E., Rao, R. M., Bansode, R. R., and Losso, J. N. (2003a). Activated carbon from pecan shell: process description and economic analysis. *Industrial Crops and Products*, 17(3):209–217.

Chilton, Marshall, W. E., Rao, R. M., Bansode, R. R., and Losso, Jacques, N. (2003b). Activated carbon from pecan shell: process description and economic analysis. *Industrial Crops and Products*, 17(3):209–217.

Dada, O. (2012). Langmuir, freundlich, temkin and dubinin–radushkevich isotherms studies of equilibrium sorption of zn 2+ unto phosphoric acid modified rice husk. *J. Appl. Chem.*, 3:38–45.

Daifullah, A., Girgis, B., and Gad, H. (2003). Utilization of agro-residues (rice husk) in small waste water treatment plans. *Materials letters*, 57(11):1723–1731.

Danish, M. and Ahmad, T. (2018). A review on utilization of wood biomass as a sustainable precursor for activated carbon production and application. *Renewable and Sustainable Energy Reviews*, 87:1–21.

De Gisi, S., Lofrano, G., Grassi, M., and Notarnicola, M. (2016). Characteristics and adsorption capacities of low-cost sorbents for wastewater treatment: A review. *Sustainable Materials and Technologies*, 9:10–40.

De Rossi, A., Rigueto, C. V., Dettmer, A., Colla, L. M., and Piccin, J. S. (2020). Synthesis, characterization, and application of saccharomyces cerevisiae/alginate composites beads for adsorption of heavy metals. *Journal of Environmental Chemical Engineering*, 8(4):104009.

Devi, K. . D. (2020). Stabilization and solidification of arsenic and iron contaminated canola meal biochar using chemically modified phosphate binders. *Journal of Hazardous Materials*, 385:121559.

Din, M. I., Hussain, Z., Mirza, M. L., Shah, A. T., and Athar, M. M. (2014). Adsorption optimization of lead (ii) using saccharum bengalense as a non-conventional low cost biosorbent: Isotherm and thermodynamics modeling. *International Journal of Phytoremediation*, 16(9):889–908.

Ding, L., Zou, B., Gao, W., Liu, Q., Wang, Z., Guo, Y., Wang, X., and Liu, Y. (2014). Adsorption of rhodamine-b from aqueous solution using treated rice husk-based activated carbon. *Colloids and Surfaces A: Physicochemical and Engineering Aspects*, 446:1–7.

Ebadi, S. M. . K. (2009). What is the correct form of bet isotherm for modeling liquid phase adsorption? *Adsorption*, 15:65–73.

El Chami, D., Daccache, A., and El Moujabber, M. (2020). What are the impacts of sugarcane production on ecosystem services and human well-being? a review. *Annals of Agricultural Sciences*, 65(2):188–199.

El-Khaiary (2008). Least-squares regression of adsorption equilibrium data: Comparing the options. *Journal of Hazardous Materials*, 158(1):73–87.

enassi, L., Bosio, A., Dalipi, R., Borgese, L., Rodella, N., Pasquali, M., Depero, L. E., Bergese, P., and Bontempi, E. (2015). Comparison between rice husk ash grown in different regions for stabilizing fly ash from a solid waste incinerator. *Journal of environmental management*, 159:128–134.

Faust, S. D. and Aly, O. M. (2013). *Adsorption processes for water treatment*. Elsevier.

Fiessinger, Richard, Y., Montiel, A., and Musquere (1981). Advantages and disadvantages of chemical oxidation and disinfection by ozone and chlorine dioxide. *Science of the Total Environment*, 18:245–261.

Freundlich, H. (1907). Über die adsorption in lösungen. *Zeitschrift für Physikalische Chemie*, 57U(1):385–470.

Fu, F. and Wang, Q. (2011). Removal of heavy metal ions from wastewaters: A review. *Journal of Environmental Management*, 92(3):407–418.

Giles, MacEwan, N. . S. (1960). 786. studies in adsorption. part xi. a system of classification of solution adsorption isotherms, and its use in diagnosis of adsorption mechanisms and in measurement of specific surface areas of solids. *J. Chem. Soc.*, pages 3973–3993.

Gopalakrishnan, C. and Nahan, M. (1977). Economic potential of bagasse as an alternate energy source: The hawaiian experience. In *Agriculture and energy*, pages 479–488. Elsevier.

Goyal, B. . (2005). *Activated Carbon Adsorption*.

Greenlee, L. F., Lawler, D. F., Freeman, B. D., Marrot, B., and Moulin, P. (2009). Reverse osmosis desalination: water sources, technology, and today's challenges. *Water research*, 43(9):2317–2348.

Gunawardene, O. H., Gunathilake, C. A., Vikrant, K., and Amaraweera, S. M. (2022). Carbon dioxide capture through physical and chemical adsorption using porous carbon materials: A review. *Atmosphere*, 13(3):397.

Gundogdu, A., Duran, C., Senturk, H. B., Soylak, M., Ozdes, D., Serencam, H., and Imamoglu, M. (2012). Adsorption of phenol from aqueous solution on a low-cost activated carbon produced from tea industry waste: equilibrium, kinetic, and thermodynamic study. *Journal of Chemical & Engineering Data*, 57(10):2733–2743.

Hamdaoui, O. (2006). Batch study of liquid-phase adsorption of methylene blue using cedar sawdust and crushed brick. *Journal of hazardous materials*, 135(1-3):264–273.

Hameed, B., Tan, I., and Ahmad, A. (2008). Adsorption isotherm, kinetic modeling and mechanism of 2, 4, 6-trichlorophenol on coconut husk-based activated carbon. *Chemical engineering journal*, 144(2):235–244.

Hashtroudi, H. (2020). Treatment of lead contaminated water using lupin straw: adsorption mechanism, isotherms and kinetics studies. *Desalination and Water Treatment*, 182:155–167.

Haug, Schmidt, N. H. S. . K. (1991). Mineralization of the sulfonated azo dye mordant yellow 3 by a 6-aminonaphthalene-2-sulfonate-degrading bacterial consortium. *Applied and environmental microbiology*, 57(11):3144–3149.

Hjaila, K., Baccar, R., Sarrà, M., Gasol, C., and Blánquez, P. (2013). Environmental impact associated with activated carbon preparation from olive-waste cake via life cycle assessment. *Journal of environmental management*, 130:242–247.

Ioannidou, O. and Zabaniotou, A. (2007). Agricultural residues as precursors for activated carbon production—a review. *Renewable and sustainable energy reviews*, 11(9):1966–2005.

Jiang, B., Zhang, Y., Zhou, J., Zhang, K., and Chen, S. (2008). Effects of chemical modification of petroleum cokes on the properties of the resulting activated carbon. *Fuel*, 87(10-11):1844–1848.

Jjagwe, J., Olupot, P. W., Menya, E., and Kalibbala, H. M. (2021). Synthesis and application of granular activated carbon from biomass waste materials for water treatment: A review. *Journal of Bioresources and Bioproducts*, 6(4):292–322.

Kalderis, D., Bethanis, S., Paraskeva, P., and Diamadopoulos, E. (2008). Production of activated carbon from bagasse and rice husk by a single-stage chemical activation method at low retention times. *Bioresource technology*, 99(15):6809–6816.

Kalpna, R., Mital, K., and Sumitra, C. (2011). Vegetable and fruit peels as a novel source of antioxidants. *Journal of Medicinal Plants Research*, 5(1):63–71.

Kao, P., Patwardhan, A., Allara, D., and Tadigadapa, S. (2008). Human serum albumin adsorption study on 62-mhz miniaturized quartz gravimetric sensors. *Analytical chemistry*, 80(15):5930–5936.

Kuang, Y., Zhang, X., and Zhou, S. (2020). Adsorption of methylene blue in water onto activated carbon by surfactant modification. *Water*, 12(2).

Kumari, P. (2017). Application of sugarcane bagasse for the removal of chromium (vi) and zinc (ii) from aqueous solution. *Int. Res. J. Eng. Technol*, 4:1670–1673.

Kurniawan, T. A., Chan, G. Y., Lo, W.-H., and Babel, S. (2006). Physico–chemical treatment techniques for wastewater laden with heavy metals. *Chemical engineering journal*, 118(1-2):83–98.

Kyzas, A. . (2014). Agricultural peels for dye adsorption: A review of recent literature. *Journal of Molecular Liquids*, 200.

Langmuir (1916). The constitution and fundamental properties of solids and liquids. part i. solids. *Journal of the American Chemical Society*, 38(11):2221–2295.

Lata, S. and Samadder, S. (2016). Removal of arsenic from water using nano adsorbents and challenges: a review. *Journal of environmental management*, 166:387–406.

Lee, C. L., H'ng, P. S., Chin, K. L., Paridah, M. T., Rashid, U., and Go, W. Z. (2019). Characterization of bioadsorbent produced using incorporated treatment of chemical and carbonization procedures. *Royal Society open science*, 6(9):190667.

Liberti, L. and Helfferich, F. G. (1963). Ion exchange (helfferich, friedrich).

Liou, T.-H. and Wu, S.-J. (2009). Characteristics of microporous/mesoporous carbons prepared from rice husk under base-and acid-treated conditions. *Journal of hazardous materials*, 171(1-3):693–703.

Liu, S.-B., Fung, B., Yang, T.-C., Hong, E.-C., Chang, C.-T., Shih, P.-C., Tong, F.-H., and Chen, T.-L. (1994). Effect of cation substitution on the adsorption of xenon on zeolite nay and on the xenon-129 chemical shifts. *The Journal of Physical Chemistry*, 98(16):4393–4401.

Liu, Y., Guo, Y., Zhu, Y., An, D., Gao, W., Wang, Z., Ma, Y., and Wang, Z. (2011). A sustainable route for the preparation of activated carbon and silica from rice husk ash. *Journal of hazardous materials*, 186(2-3):1314–1319.

Malik, P. K. (2003). Use of activated carbons prepared from sawdust and rice-husk for adsorption of acid dyes: a case study of acid yellow 36. *Dyes and pigments*, 56(3):239–249.

Malkoc, E. and Nuhoglu, Y. (2007). Potential of tea factory waste for chromium (vi) removal from aqueous solutions: Thermodynamic and kinetic studies. *Separation and purification technology*, 54(3):291–298.

Mann, A. P. (2016). Cogeneration of sugarcane bagasse for renewable energy production. *Sugarcane-Based Biofuels and Bioproducts*, pages 235–258.

McKay, H. . (2004). Sorption of copper (ii) from aqueous solution by peat. *Water, Air, and Soil Pollution*, 158:77–97.

Menya, E., Olupot, P., Storz, H., Lubwama, M., and Kiros, Y. (2018). Production and performance of activated carbon from rice husks for removal of natural organic matter from water: a review. *Chemical Engineering Research and Design*, 129:271–296.

Mohammadi, N., Mousazadeh, B., and Hamoule, T. (2021). Synthesis and characterization of nh 2-sio 2@ cu-mof as a high-performance adsorbent for pb ion removal from water environment. *Environment, Development and Sustainability*, 23:1688–1705.

Muniandy, L., Adam, F., Mohamed, A. R., and Ng, E.-P. (2014). The synthesis and characterization of high purity mixed microporous/mesoporous activated carbon from rice husk using chemical activation with naoh and koh. *Microporous and Mesoporous Materials*, 197:316–323.

Namasivayam, C. and Ranganathan, K. (1995). Removal of cd (ii) from wastewater by adsorption on “waste” fe (iii) cr (iii) hydroxide. *Water Research*, 29(7):1737–1744.

Paciullo, C. A., Horner, D. M., Hatton, K. W., and Flynn, J. D. (2010). Methylene blue for the treatment of septic shock. *Pharmacotherapy: The Journal of Human Pharmacology and Drug Therapy*, 30(7):702–715.

Petrovic, B., Gorbounov, M., and Soltani, S. M. (2022). Impact of surface functional groups and their introduction methods on the mechanisms of co2 adsorption on porous carbonaceous adsorbents. *Carbon Capture Science & Technology*, 3:100045.

Pokhrel, V. (2004). Treatment of pulp and paper mill wastewater—a review. *Science of The Total Environment*, 333(1):37–58.

Pütün, A. E., Özbay, N., Önal, E., and Pütün, E. (2005). Fixed-bed pyrolysis of cotton stalk for liquid and solid products. *Fuel Processing Technology*, 86(11):1207–1219.

Rafatullah, M., Sulaiman, O., Hashim, R., and Ahmad, A. (2010). Adsorption of methylene blue on low-cost adsorbents: a review. *Journal of hazardous materials*, 177(1-3):70–80.

Rana, M. S., Sámano, V., Ancheyta, J., and Diaz, J. (2007). A review of recent advances on process technologies for upgrading of heavy oils and residua. *Fuel*, 86(9):1216–1231.

René Schwarzenbach, Thomas Egli, T. B. H. U. v. G. and Wehrli, B. (2010). Global water pollution and human health. *Annual Review of Environment and Resources*, 35(1):109–136.

Rodriguez-Reinoso, F., Molina-Sabio, M., and González, M. (1995). The use of steam and co2 as activating agents in the preparation of activated carbons. *Carbon*, 33(1):15–23.

Rudi, N. N., Muhamad, M. S., Te Chuan, L., Alipal, J., Omar, S., Hamidon, N., Hamid, N. H. A., Sunar, N. M., Ali, R., and Harun, H. (2020). Evolution of adsorption process for manganese removal in water via agricultural waste adsorbents. *Heliyon*, 6(9):e05049.

Rudzinski et al. (1992). Chapter 12 - multisite occupancy adsorption on heterogeneous solid surfaces. In Rudzinski, editor, *Adsorption of Gases on Heterogeneous Surfaces*, pages 491–528. Academic Press, London.

Sahu, J., Acharya, J., and Meikap, B. (2010). Optimization of production conditions for activated carbons from tamarind wood by zinc chloride using response surface methodology. *Bioresource technology*, 101(6):1974–1982.

Saifuddin M, N. and Kumaran, P. (2005). Removal of heavy metal from industrial wastewater using chitosan coated oil palm shell charcoal. *Electronic journal of Biotechnology*, 8(1):43–53.

Saleem, J., Shahid, U. B., Hijab, M., Mackey, H., and McKay, G. (2019). Production and applications of activated carbons as adsorbents from olive stones. *Biomass Conversion and Biorefinery*, 9:775–802.

Sánchez-Borrego, F. J., Alvarez-Mateos, P., and García-Martín, J. F. (2021). Biodiesel and other value-added products from bio-oil obtained from agrifood waste. *Processes*, 9:797.

Sawyer, McCarty, P. (2003). *Chemistry for Environmental Engineering and Science*. McGraw-Hill series in civil and environmental engineering. McGraw-Hill Education.

Shafiq, A. . A. (2018). Removal of heavy metals from wastewater using date palm as a biosorbent: A comparative review. *Sains Malaysiana*, 47:35–49.

Shahwan, T. (2015). Lagergren equation: Can maximum loading of sorption replace equilibrium loading? *Chemical Engineering Research and Design*, 96:172–176.

Shukla, S. K., Al Mushaiqri, N. R. S., Al Subhi, H. M., Yoo, K., and Al Sadeq, H. (2020). Low-cost activated carbon production from organic waste and its utilization for wastewater treatment. *Applied Water Science*, 10:1–9.

Singh, N. . A. (2018). Water purification by using adsorbents: A review. *Environmental Technology Innovation*, 11:187–240.

Song, X. H. (2012). Development of efficient adsorbent materials for removal of toxic substances from water.

Sparks, A. . (1991). *Kinetics of Soil Chemical Reactions—A Theoretical Treatment*, chapter 1, pages 1–18. John Wiley Sons, Ltd.

Stavropoulos, G. and Zabaniotou, A. (2005). Production and characterization of activated carbons from olive-seed waste residue. *Microporous and mesoporous materials*, 82(1-2):79–85.

Tan, I., Ahmad, A., and Hameed, B. (2008). Adsorption of basic dye on high-surface-area activated carbon prepared from coconut husk: Equilibrium, kinetic and thermodynamic studies. *Journal of hazardous materials*, 154(1-3):337–346.

Tor, A., Cengeloglu, Y., Aydin, M. E., and Ersoz, M. (2006). Removal of phenol from aqueous phase by using neutralized red mud. *Journal of colloid and interface science*, 300(2):498–503.

Torres-Knoop, Poursaeidesfahani, V. . D. (2017). Behavior of the enthalpy of adsorption in nanoporous materials close to saturation conditions. *Journal of Chemical Theory and Computation*, 13(7):3326–3339. PMID: 28521093.

Unur, E. (2013). Functional nanoporous carbons from hydrothermally treated biomass for environmental purification. *Microporous and Mesoporous Materials*, 168:92–101.

Wagner, J. et al. (2001). *Membrane filtration handbook: Practical tips and hints*, volume 129. Osmonics Cambrige.

Worch (2012). *Adsorption Technology in Water Treatment: Fundamentals, Processes, and Modeling*.

Wu, F.-C., Tseng, R.-L., and Juang, R.-S. (2010). A review and experimental verification of using chitosan and its derivatives as adsorbents for selected heavy metals. *Journal of Environmental Management*, 91(4):798–806.

Yahya, M. A., Al-Qodah, Z., and Ngah, C. Z. (2015). Agricultural bio-waste materials as potential sustainable precursors used for activated carbon production: A review. *Renewable and sustainable energy reviews*, 46:218–235.

Yahya, M. H., Muhammad, J., and Hadi, A. R. A. (2012). A comparative study on the level of efficiency between islamic and conventional banking systems in malaysia. *International Journal of Islamic and Middle Eastern Finance and Management*, 5(1):48–62.

Yakout, S. M. (2014). Removal of the hazardous, volatile, and organic compound benzene from aqueous solution using phosphoric acid activated carbon from rice husk. *Chemistry Central Journal*, 8(1):1–7.

Yalçın, N. and Sevinc, V. (2000). Studies of the surface area and porosity of activated carbons prepared from rice husks. *Carbon*, 38(14):1943–1945.

Yan, S., Fang, M., Zhang, W., Zhong, W., Luo, Z., and Cen, K. (2008). Comparative analysis of co2 separation from flue gas by membrane gas absorption technology and chemical absorption technology in china. *Energy Conversion and Management*, 49(11):3188–3197.

Yang, B., Wang, Y., and Qian, P.-Y. (2016). Sensitivity and correlation of hypervariable regions in 16s rrna genes in phylogenetic analysis. *BMC bioinformatics*, 17(1):1–8.

Yang, T. C. and Zall, R. R. (1984). Absorption of metals by natural polymers generated from seafood processing wastes. *Industrial & engineering chemistry product research and development*, 23(1):168–172.

Yeganeh, M. M., Kaghazchi, T., and Soleimani, M. (2006). Effect of raw materials on properties of activated carbons. *Chemical Engineering & Technology: Industrial Chemistry-Plant Equipment-Process Engineering-Biotechnology*, 29(10):1247–1251.

Zaini, M. A. A., Zakaria, M., Alias, N., Zakaria, Z. Y., Johari, A., Setapar, S. H. M., Kamaruddin, M. J., and Yunus, M. A. C. (2014). Removal of heavy metals onto koh-activated ash-rich sludge adsorbent. *Energy Procedia*, 61:2572–2575.

Zhang, B., Han, X., Gu, P., Fang, S., and Bai, J. (2017). Response surface methodology approach for optimization of ciprofloxacin adsorption using activated carbon derived from the residue of desilicated rice husk. *Journal of Molecular Liquids*, 238:316–325.

Zhang, T., Walawender, W. P., Fan, L., Fan, M., Daugaard, D., and Brown, R. (2004). Preparation of activated carbon from forest and agricultural residues through co2 activation. *Chemical Engineering Journal*, 105(1-2):53–59.

Zietzschmann, F., Worch, E., Altmann, J., Ruhl, A. S., Sperlich, A., Meinel, F., and Jekel, M. (2014). Impact of efom size on competition in activated carbon adsorption of organic micro-pollutants from treated wastewater. *Water research*, 65:297–306.

Zondlo, J. and Velez, M. (2007). Development of surface area and pore structure for activation of anthracite coal. *Fuel processing technology*, 88(4):369–374.

Çiftçi Henden (2015). Nickel/nickel boride nanoparticles coated resin: A novel adsorbent for arsenic(iii) and arsenic(v) removal. *Powder Technology*, 269:470–480.